NPS-MR-98-004

NAVAL POSTGRADUATE SCHOOL
Monterey, California

Southern Hemisphere Application of the Systematic Approach to Tropical Cyclone Track Forecasting. Part II. Climatology and Refinement of Meteorological Knowledge Base

by

Anthony J. Bannister, Mark A. Boothe,
Lester E. Carr, III, and Russell L. Elsberry

September 1998

Prepared for: Space and Naval Warfare Systems Command
PMW 185
San Diego, CA 92110-3127

Naval Postgraduate School
Monterey, California 93943-5000

Rear Admiral Robert C. Chaplin
Superintendent

Richard Elster
Provost

This report was prepared for the Space and Naval Warfare Command (PMW 185) under Program Element 0604 207N entitled: "Systematic Approach Tropical Cyclone Forecast Techniques." The technique is intended for application at the Joint Typhoon Warning Center (JTWC) at the Naval Pacific Meteorology and Oceanography Center (NPMOC) West, Guam and for the Alternate JTWC at NPMOC, Pearl Harbor, Hawaii.

This report was prepared by:

Anthony J. Bannister by RLE
Anthony J. Bannister
Bureau of Meteorology
Perth, Australia

Mark Boothe
Mark A. Boothe
Meteorologist

Lester E. Carr III by RLE
Lester E. Carr, III
Associate Professor of Meteorology

Russell L. Elsberry
Russell L. Elsberry
Professor of Meteorology

Reviewed by:

Kenneth L. Davidson
for Carlyle H. Wash, Chairman
Department of Meteorology

Released by:

D. W. Netzer
David W. Netzer
Dean of Research

REPORT DOCUMENTATION PAGE

Form approved

OMB No 0704-0188

1. AGENCY USE ONLY (Leave blank)	2. REPORT DATE	3. REPORT TYPE AND DATES COVERED
	September 1998	Interim 12/97 – 9/98

4. TITLE AND SUBTITLE
Southern Hemisphere Application of the Systematic Approach to Tropical Cyclone Track Forecasting. Part II: Climatology and Refinement of Meteorological Knowledge Base

5. FUNDING
N0003998WRDF125

6. AUTHOR(S)
Anthony J. Bannister, Mark A. Boothe, Lester E. Carr, III, and Russell L. Elsberry

7. PERFORMING ORGANIZATION NAME(S) AND ADDRESS(ES)
Naval Postgraduate School, Department of Meteorology
589 Dyer Rd., Room 254
Monterey, CA 93943-5114

8. PERFORMING ORGANIZATION REPORT NUMBER

9. SPONSORING/MONITORING AGENCY NAME(S) AND ADDRESS(ES)
Space and Naval Warefare Systems Command
PMW 185
Sam Diego, CA 92110-3127

10. SPONSORING/MONITORING AGENCY REPORT NUMBER

11. SUPPLEMENTARY NOTES
The views expressed in this report are those of the author and do not reflect the official policy or position of the Department of Defense.

12a. DISTRIBUTION/AVAILABILITY STATEMENT
Approved for Public Release, Distribution Unlimited

12b. DISTRIBUTION CODE

13. ABSTRACT (Maximum 200 words.)

The preliminary adaptation by Bannister *et al.* (1997) of the Systematic Approach to tropical cyclone (TC) track forecasting meteorological knowledge base to the Southern Hemisphere has been extended to eight seasons (1990-91 through 1997-98), which includes 145 (90) cyclones in the South Indian (Pacific) region. A total of 3257 synoptic pattern/region classifications could be described in the context of only four synoptic patterns and 11 synoptic regions. Updated track summaries in each pattern/region combination, and the recurring (more than three) environment structure transitions are provided.

Refinements in the set of TC-environment transitional mechanisms in the meteorological knowledge base include: (i) new Equatorial Westerly Wind Burst Mechanism; (ii) new semi-direct TC interaction equatorward conceptual model; (iii) additional variations of the Subtropical Ridge Modulation mechanisms; and (iv) further cases of Vertical Wind Shear leading to dramatic TC track changes. These refinements are illustrated with case studies intended to assist the forecaster in recognizing these transitional mechanisms, and thus anticipating TC track changes in the Southern Hemisphere.

14. SUBJECT TERMS	15. NUMBER OF PAGES
Tropical cyclone track forecasting; Tropical cyclone motion	68
	16. PRICE CODE

17. SECURITY CLASSIFICATION OF REPORT	18. SECURITY CLASSIFICATION OF THIS PAGE	19. SECURITY CLASSIFICATION OF ABSTRACT	20. LIMITATION OF ABSTRACT
UNCLASSIFIED	UNCLASSIFIED	UNCLASSIFIED	

Table of Contents

		page
Report Documentation Page		iii
Table of Contents		iv
Acknowledgments		v
List of Figures		vi
1.	Introduction	1
	a. Background	1
	b. Objectives of this study	5
2.	Expanded Climatology	6
	a. Procedures	6
	b. Expanded data base	7
	c. Standard (S) synoptic pattern	7
	d. Poleward (P) synoptic pattern	14
	e. High-amplitude (H) synoptic pattern	16
	f. Multiple (M) TC synoptic pattern	20
	g. Environment structure transition summary	21
3.	Refinement of the Meteorological Knowledge Base	27
	a. Background	27
	b. Equatorial westerly wind burst transitional mechanism	27
	1. EWWB model description	27
	2. EWWB model illustrations	28
	c. Tropical cyclone interaction-related refinements	40
	1. Semi-direct tropical cyclone interaction equatorward (STIQ) and poleward (STIP) conceptual model	40
	2. STIQ model illustration	42
	d. Subtropical ridge modification (SRM) refinements	45
	1. SRM weakening	46
	2. SRM amplifying	50
	e. Vertical wind shear illustration	50
	f. Summary	58
4.	Summary and Conclusion	
APPENDIX		63
REFERENCES		68
DISTRIBUTION LIST		69

Acknowledgments

This research has been sponsored by the Space and Naval Warfare Systems Command (SPAWAR) as a continuation of a cooperative agreement between the Naval Postgraduate School and the Australian Bureau of Meteorology. A second three-month visit by Tony Bannister of the Perth, Western Australia office was arranged. The Bureau of Meteorology funded the salary and this SPAWAR contract paid the travel and per diem to facilitate this exchange. Best-track tropical cyclone records were provided by the Joint Typhoon Warning Center, Guam, and NOGAPS analyses were provided by the Fleet Numerical Meteorology and Oceanography Center. Bob Creasey assisted in recovering NOGAPS analyses missing from the NPS archive for four tropical cyclones during 1994-1997. Mrs. Penny Jones expertly typed the manuscript.

List of Figures

Page

Fig. 1 Summary of the meteorological knowledge base of the Systematic Approach adapted for Southern Hemisphere tropical cyclones as in Bannister *et al.* 1997, except as updated in Section 3b. 2

Fig. 2 Summary of the four synoptic patterns and associated synoptic regions for the Systematic Approach meteorological knowledge base in the Southern Hemisphere. 3

Fig. 3 Summary of TC tracks from JTWC during the 1990-1991 through the 1997 – 1998 seasons in the Southern Hemisphere. 8

Fig. 4 Percent of synoptic pattern/regions in the (a) 2123 cases in the South Indian Ocean and (b) 1134 cases in the South Pacific Ocean during the 1990-1991 through 1997-1998 seasons. 10

Fig. 5 Tracks as in Fig. 3, except only while TC was in the Standard (S) pattern and (a) Equatorial Westerlies (EW) or (b) Dominant Ridge (DR) regions. 11

Fig. 5 (continued) Tracks in S Pattern and (c) Weakened Ridge (WR) and (d) Midlatitude Westerlies (MW) regions. 12

Fig. 6 Tracks as in Fig. 3, except only while the TCs are in the Poleward/Poleward -Oriented (P/PO) synoptic pattern/region. 15

Fig. 7 Tracks as in Fig. 3, except only for TCs while in the High-amplitude (H) synoptic pattern and (a) Ridge Equatorward (RE) and (b) Ridge Poleward (RP) regions. 18

Fig. 7 (continued) Tracks in H synoptic pattern for the (c) Equatorial Westerlies (EW) and (d) Trough Poleward (TP) regions. 19

Fig. 8 Tracks as in Fig. 3, except only while the TCs are in the (a) M/Equatorward Flow (EF) and (b) M/Poleward Flow (PF) pattern/regions. 22

Fig. 9 Recurring (greater than three) environment structure transitions for the (a) 145 TCs in the South Indian Ocean and (b) 90 TCs in the South Pacific Ocean (b) during 1990-1991 through 1997-1998 seasons. 24

Fig. 10 Conceptual model of Equatorial Westerly Wind Burst (EWWB) transitional mechanism. 29

Fig. 11 Best tracks of the western TC Val (0692) and the eastern TC Wasa (0792) during 00 UTC 5 December to 00 UTC 11 December 1991. 29

Fig. 12 Geostationary Meteorological Satellite infrared imagery at (a) 03 UTC 6 December and (b) 03 UTC 9 December 1991. 30

Page

Fig. 13 NOGAPS 500-mb analysis valid at (a) 12 UTC 6 December 1991 and (b) 00 UTC 9 December. 32

Fig. 14 (a) NOGAPS 500-mb analysis as in Fig. 13, except valid at 00 UTC 13 November 1991, and (b) the GMS IR imagery at 03 UTC 13 November 1991. 33

Fig. 15 (a) NOGAPS 500-mb analysis as in Fig. 13, except at 00 UTC 14 November 1991, and the (b) GMS IR imagery at 03 UTC 14 November 1991. 35

Fig. 16 Best track as in Fig. 11, except for TC Lena (1393) between 00 UTC 27 January 1993 and 00 UTC 2 February. 36

Fig. 17 (a) NOGAPS 500-mb analysis as in Fig. 13, except valid at 12 UTC 27 January, (b) 28 January, (c) 29 January, and (d) 31 January 1993. 37

Fig. 17 (continued) (c) NOGAPS 500-mb analysis valid at 12 UTC 29 January and 00 UTC 31 January 1993. 38

Fig. 18 Conceptual model as in Fig. 10, except for the Semi-direct TC Interaction (STI) involving the equatorward TC (STIQ) with the equatorial Buffer (B) cell, or involving the poleward TC (STIP) with the subtropical Anticyclone (A). 41

Fig. 19 Best tracks as in Fig. 11, except for the equatorward TC Nina (0693) and the poleward TC Kina (0793) during 12 UTC 31 December 1992 to 12 UTC 4 January 1993. 41

Fig. 20 NOGAPS 500-mb analyses as in Fig. 13, except valid at 12 UTC (a) 1 January, (b) 2 January, and (c) 3 January 1993. 43

Fig. 20 (continued) panel (c). 44

Fig. 21 GMS IR imagery 03 UTC on (a) 1 January, (b) 2 January, and (c) 3 January 1993. 44

Fig. 22 Best track as in Fig. 11, except for TC Alexandra (0992) during 00 UTC 20 December to 00 UTC 26 December 1991. 46

Fig. 23 NOGAPS 500-mb analyses as in Fig. 13, except valid at 00 UTC on (a) 21, (b) 22, (c) 23, and (d) 24 December 1991. 47

Fig. 24 Best track as in Fig. 11, except for TC Besty (0392) during 5-10 January 1992. 51

Fig. 25 NOGAPS 500-mb analyses as in Fig. 13, except valid at 12 UTC on (a) 7, (b) 8, and (c) 9 January 1992. 51

Page

Fig. 25 (continued) NOGAPS 500-mb analyses on (b) 8, and (c) 9 January 1992. 52

Fig. 26 Best track as in Fig. 11, except for TC Tia (0392) during 12 UTC 18 November to 12 UTC 21 November 1991. 54

Fig. 27 NOGAPS 500-mb analyses as in Fig. 13, except at 12 UTC on (a) 19 and (b) 20 November 1991. 55

Fig. 28 NOGAPS analyses as in Fig. 13, except at 200 mb for 12 UTC on (a) 19, and (b) 20 November 1991, and at 850 mb in (c) and (d) for the same dates. 56

Fig. 28 (continued) NOGAPS 500-mb analyses at 12 UTC on (c) 19 and (d) 20 November 1991. 57

1. Introduction

a. Background

Bannister *et al.* (1997) examined the possible adaptation of the Systematic Approach to Tropical Cyclone Track Forecasting (hereafter Systematic Approach) meteorological knowledge base to the Southern Hemisphere (Fig. 1). The environment structure conceptual models of the Systematic Approach that Carr and Elsberry (1994) originally developed for the western North Pacific were applied to all South Indian Ocean and South Pacific tropical cyclones (TCs) during January 1994 – June 1997. Since the dividing line between these basins was defined to be 142°E, all of the TCs in the Gulf of Carpentaria and Arafura or Timor Seas were designated as being in the South Indian Ocean. The Systematic Approach environment structure assignments were based on the U. S. Navy Operational Global Atmospheric Prediction System (NOGAPS) analyses and the Joint Typhoon Warning Center (JTWC), Guam, best tracks (post-season analyses). Monthly catalogues of Geostationary Meteorological Satellite (GMS) full-disk visible and infrared imagery once a day at 03 UTC were available. After October 1995, a GMS water vapor image was also included in the catalogues. Some of the central Indian Ocean TCs were on the edge of the GMS image and thus were not well resolved. No Meteosat imagery was available for the western Indian Ocean TCs.

Bannister *et al.* (1997) classified 1592 cases during the 1994-97 period into four synoptic patterns and 11 synoptic regions (Fig. 2). Whereas three of the four synoptic patterns from the western North Pacific could be applied with relatively small modifications, a new High-amplitude (H) synoptic pattern was defined to classify situations with large penetrations of midlatitude troughs and ridges deep into the Southern Hemisphere (SH) tropics. A new Equatorial Westerlies (EW) synoptic region was defined in the H and Standard (S) synoptic

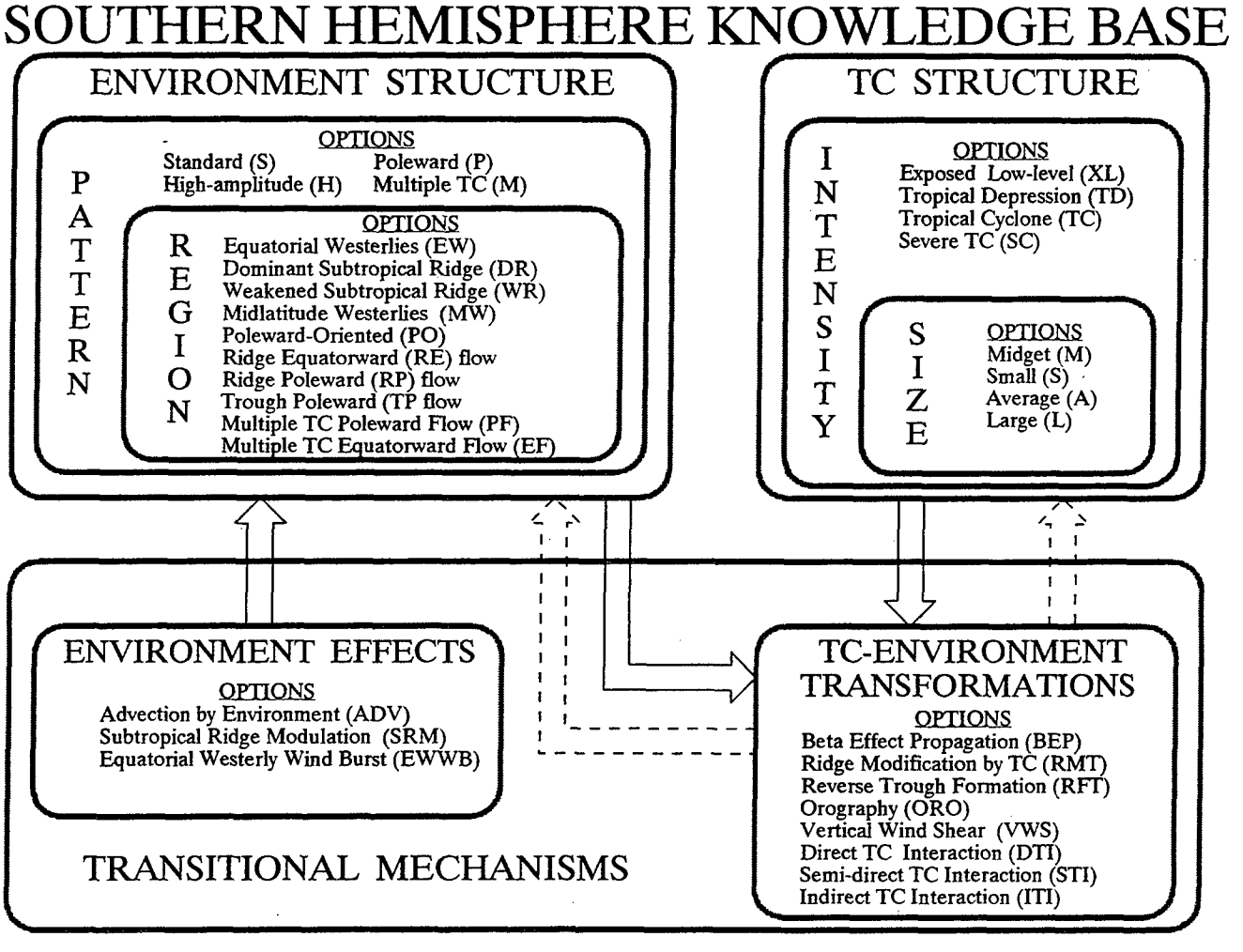

Fig. 1 Summary of the meteorological knowledge base of the Systematic Approach adapted for Southern Hemisphere tropical cyclones as in Bannister *et al.* (1997), except as updated in Section 3b. See text for definitions and descriptions of these components.

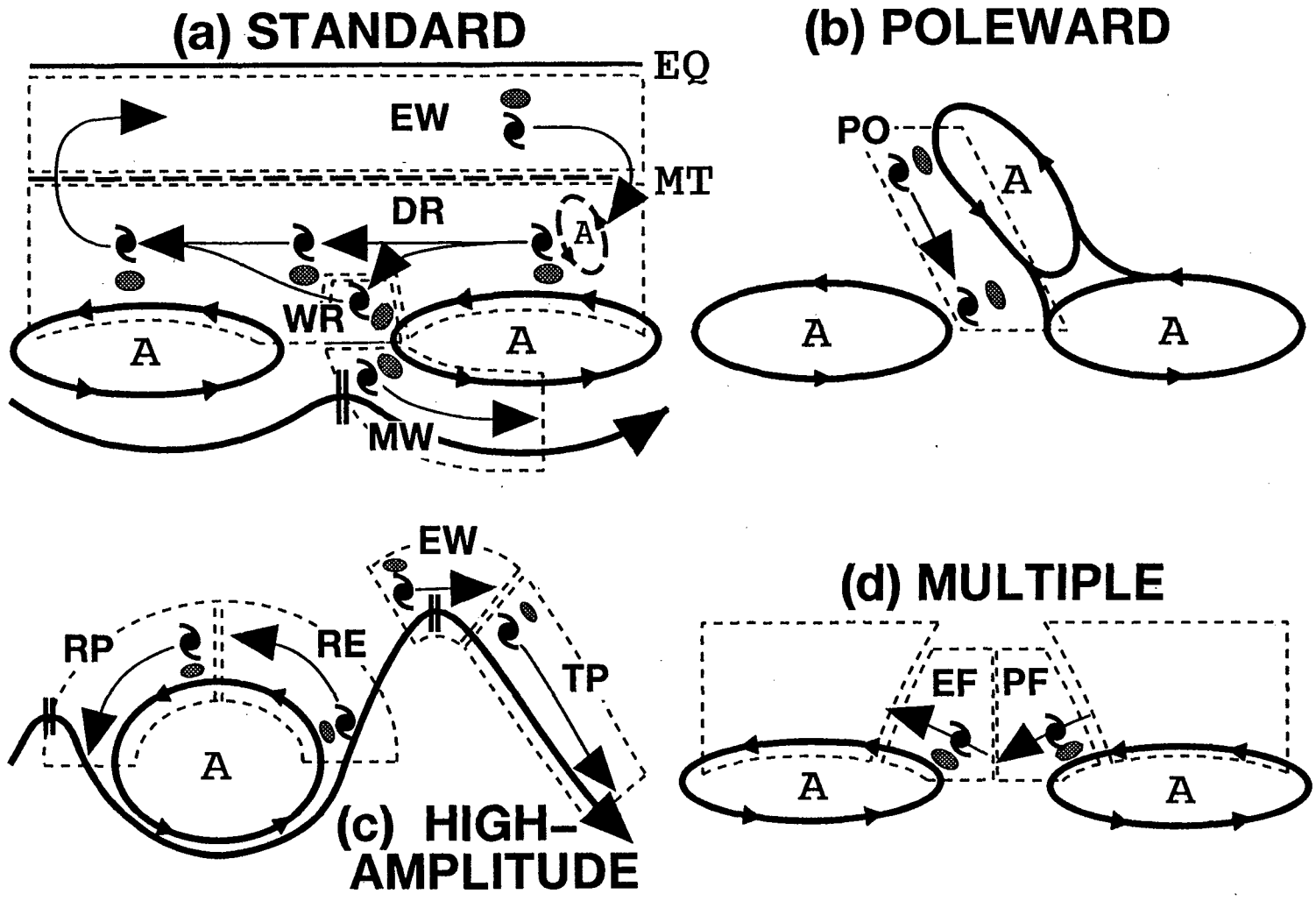

Fig. 2 Summary of the four synoptic patterns and associated synoptic regions for the Systematic Approach meteorological knowledge base in the Southern Hemisphere (Bannister *et al.* 1997). The symbols EQ, MT, and A are for Equator, Monsoon Trough, and Anticyclone.

patterns to account for low latitude SH storms that track toward the east. Other new synoptic regions in the H pattern are the Ridge Poleward (RP), Ridge Equatorward (RE), and the Trough Poleward (TP), wherein the orientation and magnitude of the TC track vectors are primarily determined by the meridionally oriented ridge or trough, respectively. However, the pressure gradient between the primary ridge (trough) and the adjacent trough (ridge) determines th strength of the environmental steering of the TC. Other aspects of the S, Poleward (P), a Multiple (M) synoptic patterns in Fig. 2 were found to apply in the SH as in the western h Pacific, or in the eastern/central North P fic region application of the Systematic Appr by Boothe (1997).

Examples from the NOGAPS analyses of the synoptic pattern/regions for the SH given in Bannister *et al.* (1997). They also provide track summaries for each pattern/regi based on the 1994—97 period. Preliminary climatologies of synoptic patterns and synoptic regions based on this period were also presented for the combined South Indian and Pacific sample of 1592 cases.

Each of the TC-environment transformations (Fig. 1, lower right) originally defined for Northern Hemisphere TCs were also found by Bannister *et al.* (1997) to apply in the SH sample. In particular, three TC interactions (Direct, Semi-direct, and Indirect) defined in a recent paper (Carr *et al.* 1997) were adapted for SH application. Series of NOGAPS analyses and tracks during TC interactions in the SH were provided in Bannister *et al.* (1997). An objective technique for detecting certain TC interactions developed by Carr and Elsberry (1998) for the western North Pacific was modified for SH geometry of tracks and provided useful guidance.

As long as a TC remains in the environmental steering flow associated with a particular synoptic pattern and region, the motion of the TC will tend to fall within a certain range of

directions and speeds, i.e., in a characteristic track. A TC may remain in the same pattern/region combination throughout its existence, e.g., straight-running TCs in the tradewinds equatorward of the subtropical ridge are classified in the S/Dominant Ridge (DR) pattern/region. However, a majority of TCs have more complex tracks owing to changes in the environment structure of the TC, which are called "transitions" in the Systematic Approach. The associated transitional mechanisms are given in the bottom half of Fig. 1. Bannister *et al.* (1997) summarized the frequency of the environment structure transitions based on the 1994-97 period. They also presented a series of mini-case studies using NOGAPS analyses and JTWC tracks to illustrate the more frequently occurring transitions.

b. *Objectives of this study*

The primary objective of this study was to expand the sample of SH storms beyond that of Bannister *et al.* (1997) to establish a firmer basis for application of the Systematic Approach. Thus, the most recent (1997-98) season and three earlier seasons (1990-91, 1991-92, 1992-93) will be added to the data base to create an eight-year sample. Revised climatologies of pattern/region frequencies, track summaries, and environment structure transitions will be presented in Section 2. During the classification of the expanded sample, certain refinements of the meteorological knowledge base in Fig. 1 were made. These refinements will be described in Section 3.

2. Expanded Climatology

a. Procedures

The approach in this study follows that described by Bannister *et al.* (1997). That is, NOGAPS analyses with the JTWC best-track positions at +12, 00, -12, -24, and –36 h were used to indicate the track orientation relative to the synoptic calculations. All NOGAPS analyses prior to June 1994 were for a Triangular (T) 79 resolution, compared to the doubled (T 159) resolution following that date. Since the objective is a synoptic environment classification, the coarser resolution of the earlier NOGAPS analyses was usually not a problem. Cases of poorly defined circulations were found in both resolutions that are more associated with data sparsity issues. Advantages of hindsight allow resolution of questionable situations in this research setting that would be more difficult in operations. Team discussions were used to resolve a number of ambiguous situations to obtain the best possible data base of environmental structure classifications. It is emphasized again for this new sample that a "storyline" for each storm track could be defined in the context of only four synoptic patterns and 11 synoptic regions (Fig. 2).

The catalogued GMS imagery was again the only source of satellite imagery in the earlier three years and thus imagery was unavailable in the western Indian Ocean. However, Meteosat imagery was available over this region during the 1997-98 season.

In the Bannister *et al.* (1997) study, the objective TC interaction (TCI) program of Carr and Elsberry (1998) had been provided in advance to the classifier as an alert to potential situations. Having gained experience with the TCI conceptual models adapted for the SH (Fig. 5 of Bannister *et al.*), these new classifications have been made without having the objective TCI technique available. In the second iteration, the TCI cases flagged by the objective technique were checked for consistency with the unaided classifications. This procedure served as a more

independent test that the objective TCI program modified for SH application is indeed useful. An extension of the TCI conceptual model will be presented in Section 3.

b. Expanded data base

The inclusion of the additional four years of cases essentially doubled the sample of environment structure classifications by Bannister *et al.* (1997). Four additional TCs during the 1994-97 period for which NOGAPS analyses had not previously been available were added as well. Thus, the total number of classifications was 3257, with 2123 cases in the South Indian Ocean and 1134 cases in the South Pacific Ocean. Bannister *et al.* had analyzed 1592 cases. The 1991-1998 (only the second year is used as a designator, i.e., 1991 includes the 1990-91 season and 1998 refers to 1997-98 season) sample includes 145 (90) TCs in the South Indian (Pacific) region, which includes seven TCs that crossed 142° E and thus were counted in both regions.

The tropical cyclone tracks for the 1991-98 sample are given in Fig. 3, and may be compared with those for the 1994-97 sample in Fig. 4 of Bannister *et al.* (1997). Although the same general track characteristics are found in each sample, the coverage is clearly much improved. Although the same characteristic clustering of the tracks between about 8°S and 25°S is found, a more broad distribution of tracks extending to 40°S is present in the larger sample. Inclusion of the 1997-98 El Niño period increased the sample of South Pacific storms and the tracks now extend to about 130°W (versus about 150°W in prior sample). Specific tracks in the synoptic patterns and regions will be presented below.

c. Standard (S) synoptic pattern

This S synoptic pattern and the associated synoptic regions are illustrated in Fig. 2a. The S pattern constitutes 66.1% of all of the 12-h pattern classifications in the South Indian Ocean

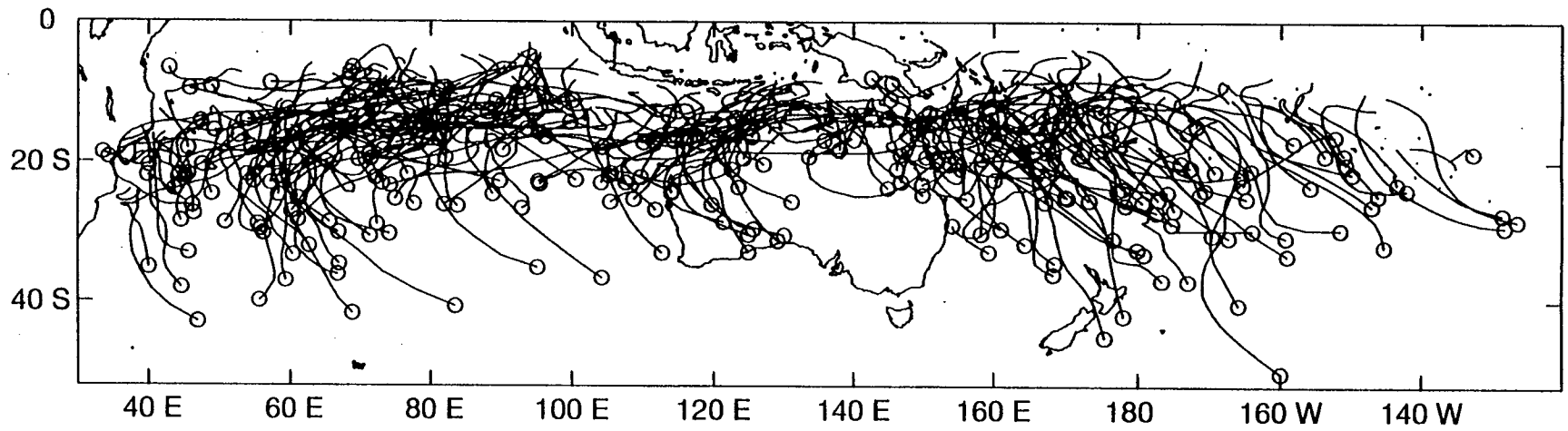

Fig. 3 Summary of TC tracks from JTWC during the 1990-1991 through the 1997 – 1998 seasons in the Southern Hemisphere. The ending position is indicated with a circle.

(Fig. 4a), and 54.5% in the South Pacific Ocean (Fig. 4b). Analysis examples of this synoptic pattern are given in Section 3a of Bannister *et al.* (1997).

The tracks in the S/Equatorial Westerlies (EW) pattern/region during 1991-98 are shown in Fig. 5a. This larger sample indicates a broader longitudinal range of S/EW occurrences than did the earlier sample. Nevertheless, most of the cases are in the band from 90°E to just east of the dateline, which is a region where the monsoon equatorial westerlies are favored. Many of these S/EW tracks are very short, which suggests the time that a TC may remain in this pattern/region is not very long. However, a few storms have longer periods in S/EW. Overall, the 12-h analyses in the S/EW pattern/region constitute only 6.0% of the South Indian Ocean classifications (Fig. 4a) during 1991-98, and 12.1% for the South Pacific region (Fig. 4b). Since the number of individual S/EW storms in the South Indian Ocean is almost the same as in the South Pacific Ocean, the larger percentage for the latter basin arises because of the longer tracks (Fig. 5a).

The most common of all pattern/region combinations is the S/Dominant Ridge (DR), which is a westward track equatorward of the subtropical anticyclone (Fig. 2a). In the South Indian Ocean, 50.8% of all classifications are in the S/DR pattern/region (Fig. 4a). While not as frequent in the South Pacific Ocean, still 24.3% are found in the S/DR (Fig. 4b). This difference in frequency is well illustrated by the 1991-98 track summary (Fig. 5b). Long tracks to the west are found in the S/DR pattern/region of the South Indian Ocean. Although some long westward tracks are also found in the South Pacific Ocean, the number and areal extent of S/DR tracks is smaller than in the South Indian Ocean. Most of these S/DR tracks are clustered between 10°S and 25°S, so a considerable overlap exists with the latitudinal band in which eastward S/EW tracks are found (Fig. 5a).

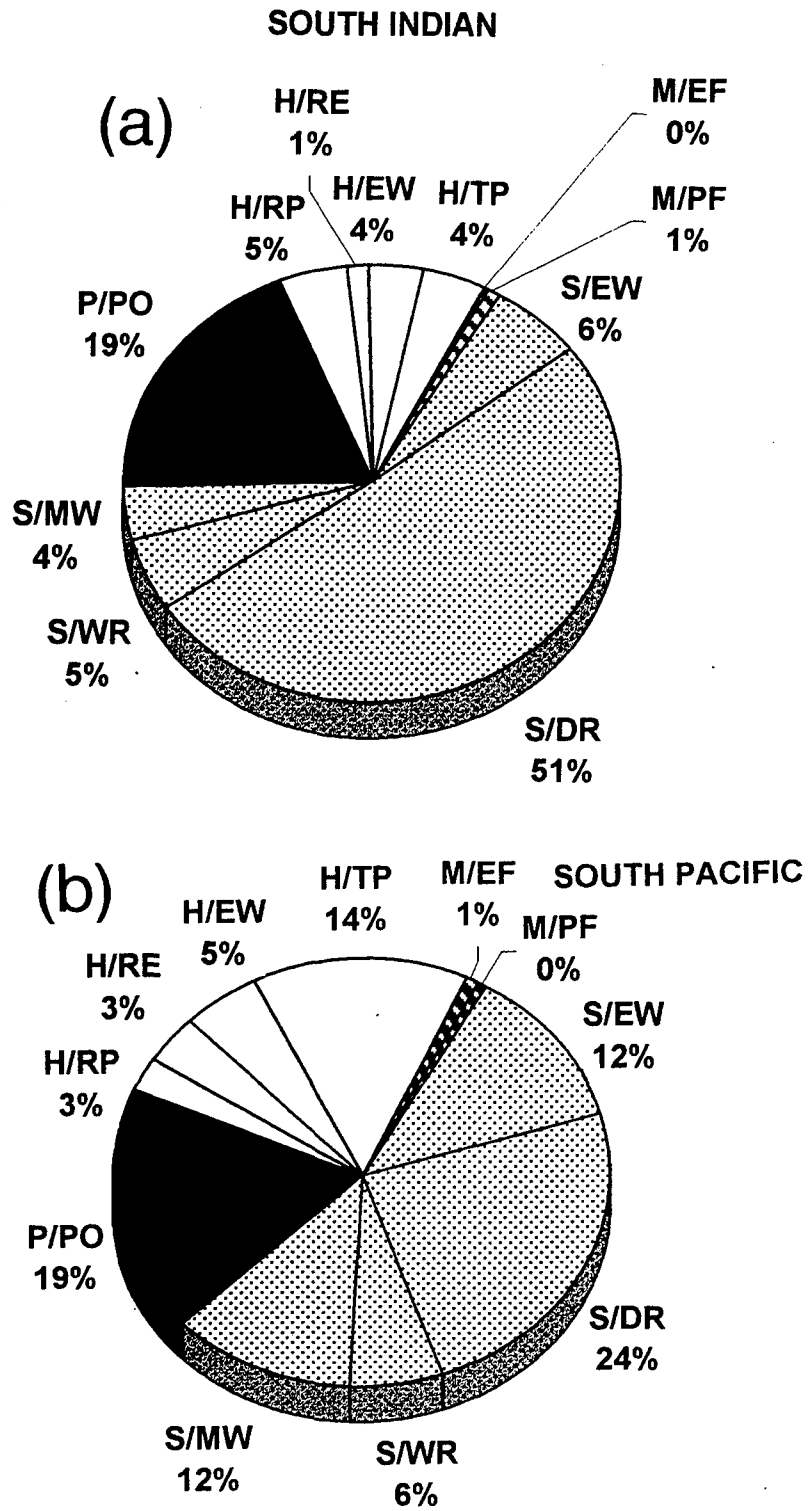

Fig. 4 Percent of synoptic pattern/regions in the 12-h analyses for (a) 2123 cases in the South Indian Ocean and (b) 1134 cases in the South Pacific Ocean during the 1990-1991 through 1997-1998 seasons.

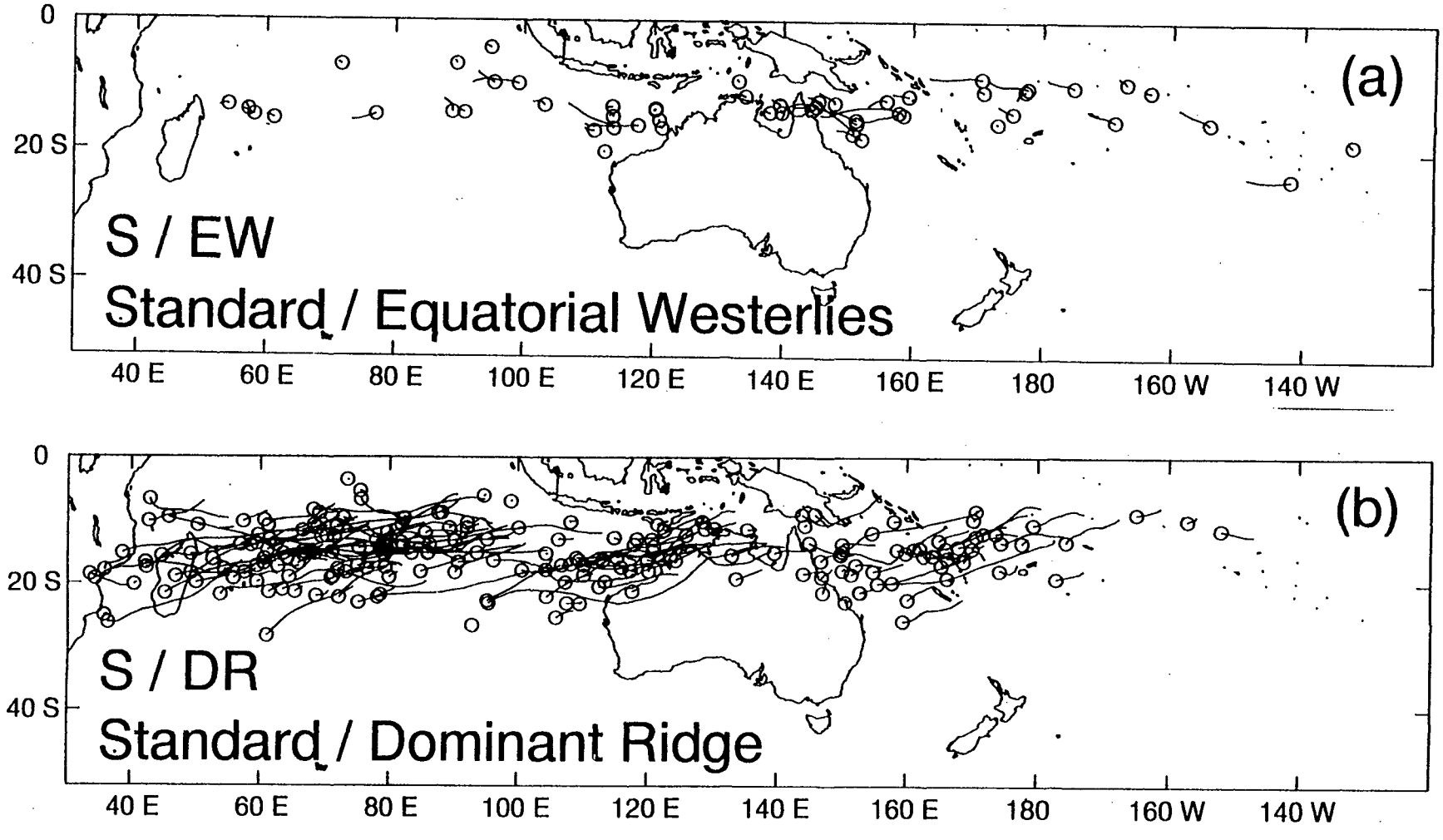

Fig. 5 Tracks as in Fig. 3, except only while TC was in the Standard (S) pattern and (a) Equatorial Westerlies (EW) or (b) Dominant Ridge (DR) regions.

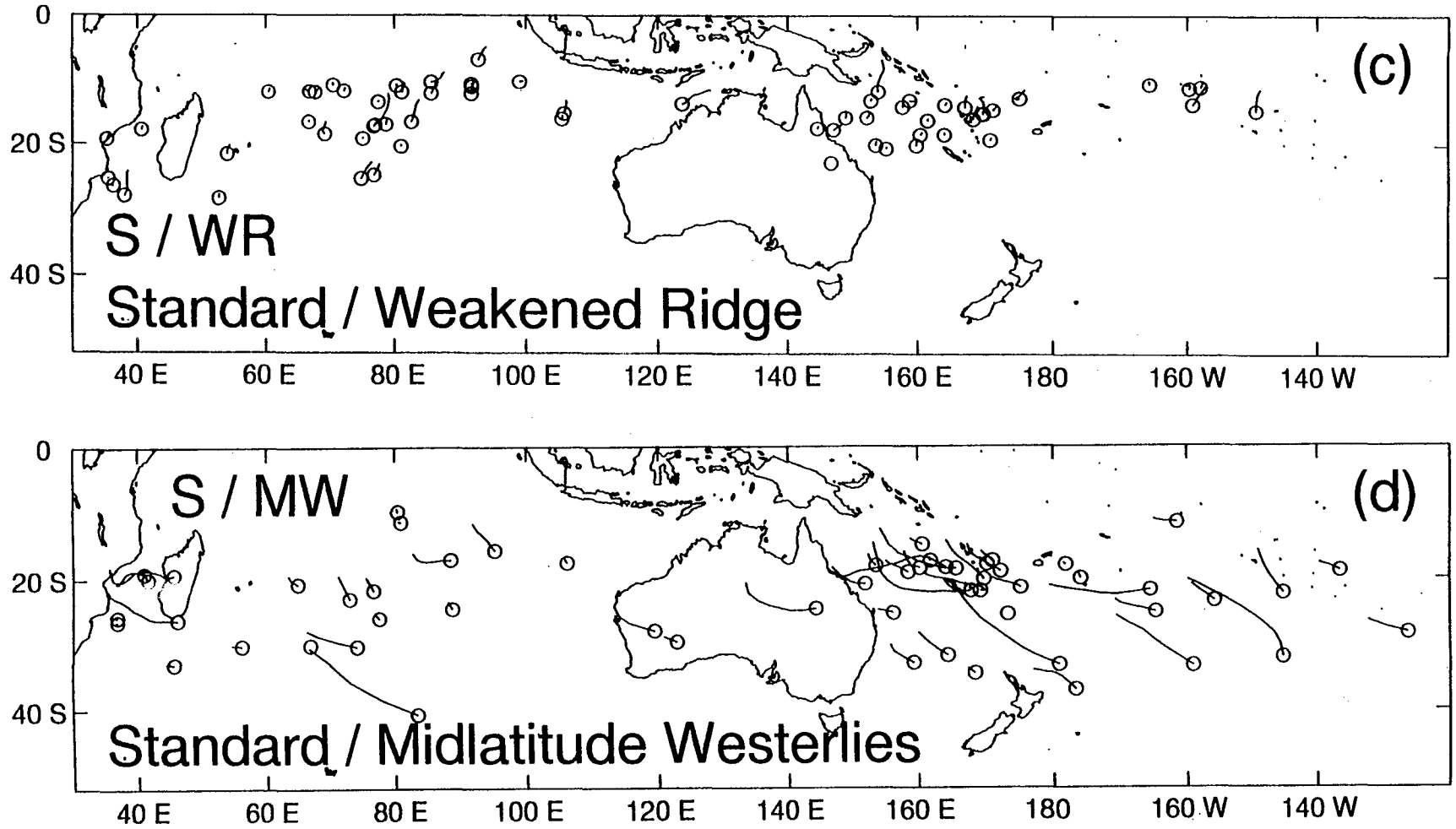

Fig. 5 (continued) Tracks in S pattern and (c) Weakened Ridge (WR) and (d) Midlatitude Westerlies (MW) regions so a considerable overlap exists with the latitudinal band in which eastward S/EW tracks are found (Fig. 5a).

As shown in Fig. 2a, the Weakened Ridge (WR) synoptic region is a small area in which TCs turn poleward from a westward track in S/DR toward a recurvature through the subtropical ridge. Because of the small area and short time that a TC typically stays in S/WR, the percentages of 12-h classifications in this pattern/region are only 5.4% and 6.1% in the South Indian and Pacific Oceans (Figs. 4a and 4b). As illustrated in Fig. 5c, almost all of the S/WR tracks are very short with a poleward and slightly westward orientation.

As the Midlatitude Westerlies (MW) region title implies, TCs in this MW region are in eastward environmental steering (Fig. 2a). By definition, TCs in S/MW have recurved so that the tracks are southward and eastward (Fig. 5d). The three tracks near 10°S occurred during the early season when the SH westerlies are quite close to the Equator. Whereas the western North Pacific TCs in S/MW generally have long post-recurvature tracks (Carr *et al.* 1995), the South Indian Ocean storms have surprisingly short tracks as these TCs rapidly dissipate. More TCs with longer tracks in S/MW are found over the South Pacific, including eight TCs that continued to about 35°S. Given these differences in the number of TCs with long tracks, it is not surprising that the frequency of 12-h analyses with a TC in S/MW is only 4.0% in the South Indian Ocean (Fig. 4a) and 12.0% in the South Pacific Ocean (Fig. 4b).

By definition, the environmental steering flows in the same synoptic region within the S pattern are similar in the South Indian and South Pacific Oceans, so that similar characteristic TC tracks are still found in each basin (Fig. 5). However, the larger 1991-98 sample illustrates with more confidence that the frequencies of occurrence of the S synoptic regions are rather different between the two regions. Based on a western North Pacific study (Carr *et al.* 1995) that demonstrated different degrees of difficulty in forecasting tracks in various synoptic

pattern/region combinations, comparisons of track forecasting performance between the two basins should be made carefully considering that degree of difficulty for each sample of forecasts.

d. Poleward (P) synoptic pattern

The conceptual model of the P synoptic pattern for the SH (Fig. 2b) is a direct reflection of the original model from the western North Pacific (Carr and Elsberry 1994). Key features are a significant break in the subtropical anticyclone poleward of the TC, and a prominent, primarily poleward-oriented anticyclone to the east that extends equatorward of the TC. As Bannister *et al.* (1997) illustrate with synoptic NOGAPS analyses, a climatologically favored SH region for such a P pattern is the SPCZ, which is a favored region for TC development and serves as a background poleward steering flow. A peripheral anticyclone to the north and east in the Rossby wave dispersion that trails larger TCs may then provide an additional contribution to the poleward motion.

Only the one Poleward-Oriented (PO) synoptic region is defined in the P pattern for the SH (Fig. 2b). That is, a P/MW is not defined as in the western North Pacific, as SH storms that have an environmental steering controlled by the midlatitude westerlies are said to have transitioned to S/MW (Fig. 2a; tracks in Fig. 5d). As indicated in Figs. 4a and 4b, this P/PO pattern/region is rather common, with 19.1% and 18.8% of all 12-h analyses in the South Indian Ocean and South Pacific Ocean, respectively. The TC tracks in P/PO during 1991-98 (Fig. 6) are similar to those during 1994-1997 (Bannister *et al.* 1997, Fig. 12), except that a broader longitudinal distribution is found. One P/PO storm is now moving poleward along 140°W, whereas the eastern-most P/PO track in the earlier sample was along 165°W. Although more

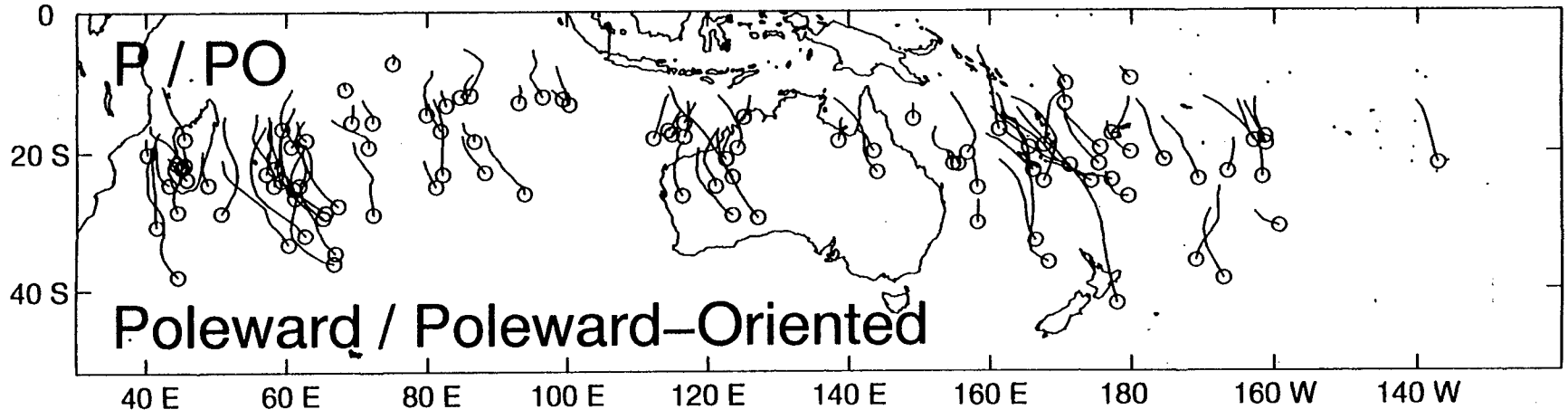

Fig. 6 Tracks as in Fig. 3, except only while the TCs are in the Poleward/Poleward Oriented (P/PO) synoptic pattern/region.

P/PO tracks are now found in the central South Indian Ocean, a similar tendency is evident for three track clusters in the western Indian Ocean, over West Australia, and 160°E - 160°W. Notice also that a large majority of these TCs turn poleward in the 15°-20°S band. Many of these tracks into the midlatitudes are quite long, especially relative to the S/MW tracks in Fig. 5d. Many of these tracks terminate in the 25°S - 30°S band, which may be because the TCs dissipated. An alternative that will be documented later is that they may have had a transition to other poleward-moving tracks (either S/MW or H/TP, see Fig. 2), or have returned to a westward track in S/DR. A few P/PO tracks do persist to 40°S, which suggests these TCs did not experience destructive vertical wind shear while in the P/PO pattern/region.

e. *High-amplitude (H) synoptic pattern*

As in Bannister *et al.* (1997), the most important difference in the environment structure of SH TCs from the western North Pacific TCs addressed in the original Systematic Approach application arises from the more vigorous intrusions of midlatitude trough/ridge systems deep into the SH tropics. That is, the subtropical anticyclone from the coast of Africa to the Central South Pacific is highly transient, often has more circular cells, is frequently disrupted by midlatitude trough/ridge systems that are usually tilted NW-SE, and is weak compared to the western North Pacific. Thus, a new High-amplitude (H) synoptic pattern (Fig. 2c) was introduced to describe fully this conceptual model and provide case studies with NOGAPS analayses. The new eight-year sample provides better statistics on the frequency of the occurrence of the H pattern/regions in both the South Indian Ocean (Fig. 4a) and South Pacific Ocean (Fig. 4b).

Any equatorward deflection of a TC is usually considered anomalous in view of the tendency for the beta-effect propagation to contribute to poleward motion of cyclonic vortices.

An environmental steering that has such an equatorward component is the Ridge Equatorward (RE) synoptic region in the H pattern (Fig. 2c). With the more transient subtropical anticyclone in the SH, the TC is typically in the H/RE pattern/region because the subtropical anticyclone has built eastward poleward of a low-latitude TC and caused an environmental steering that is equatorward of west. Another scenario that led to a H/RE pattern/region via vertical wind shear will be described in Section 3e. This case of TC Tia was the origin of the longest H/RE track toward the northwest in Fig. 7a. Whereas the four-year sample of Bannister et al. (1997) had contained only four cases, the new eight-year sample would suggest an average of two occurrences per year. In the South Pacific (Indian) Ocean, the percent of 12-h analyses in the H/RE pattern/region was 3.4% (1.4%)

The Ridge Poleward (RP) region of the H pattern is more frequently found in the South Indian Ocean than in the South Pacific Ocean (Fig. 7b). This pattern/region appears to be quite important along the northwest coast of Australia, and leads to poleward motion that can threaten coastal communities. Overall, the short tracks in Fig. 7b would suggest limited periods that the TC is on the "shoulder" of a meridional ridge in the H pattern. However, a few longer H/RP tracks, and thus more persistent circulation scenarios, are also present in Fig. 7b. Such track variability will make forecasting of these cases rather difficult. Based on the 1991-98 sample (Fig. 4), the H/RP occurrences are 4.5% and 2.6% in the South Indian and South Pacific Oceans, respectively.

A unique pattern/region in the SH is the H/EW at the equatorward end of a deeply penetrating midlatitude trough (Fig. 2c). This is the reason for many eastward TC tracks in the 10° - 20° lat. band (Fig. 7c) that in other basins would be expected to have westward tracks.

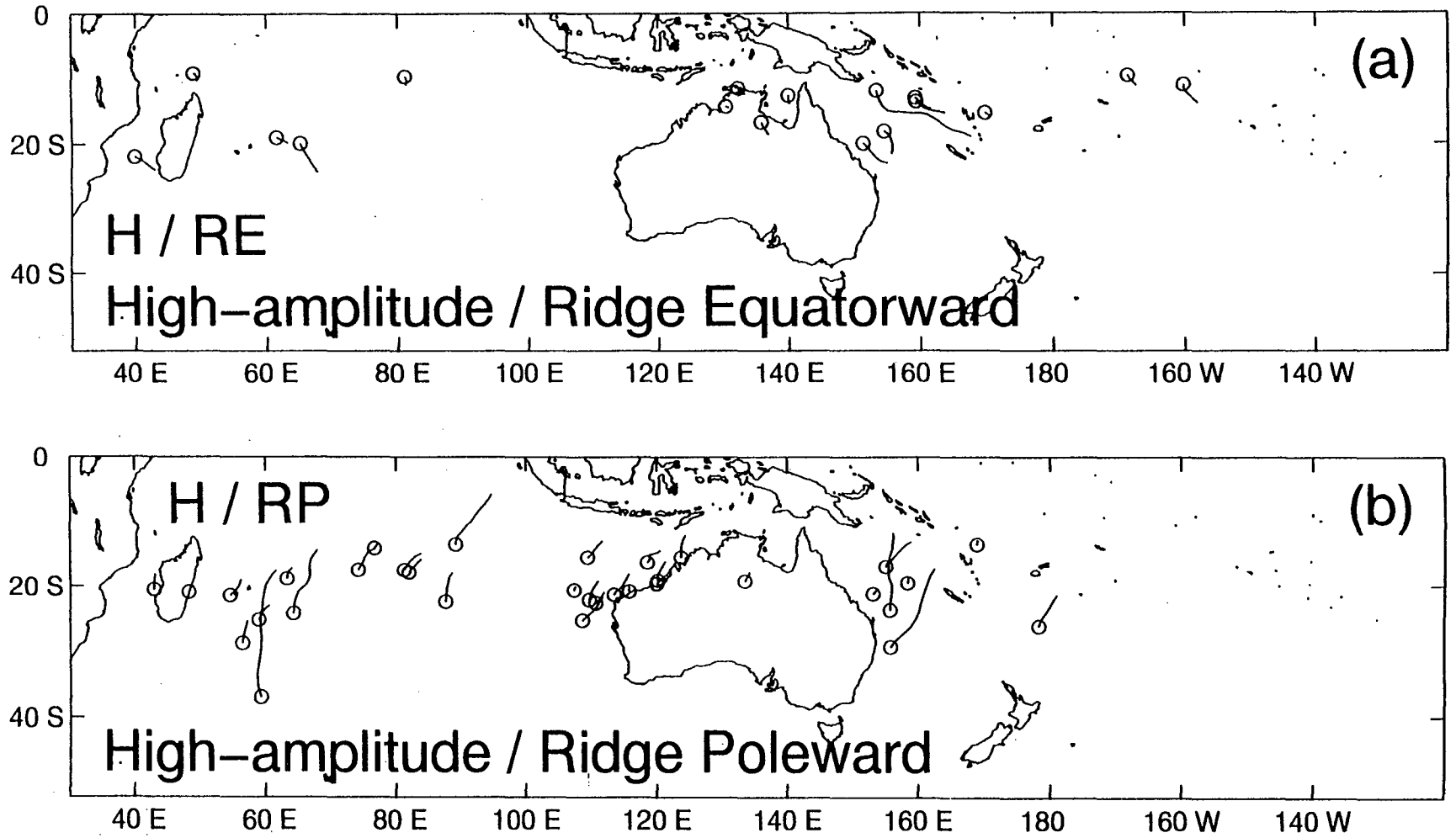

Fig. 7 Tracks as in Fig. 3, except only for TCs while in the High-amplitude (H) synoptic pattern and (a) Ridge Equatorward (RE) and (b) Ridge Poleward (RP) regions.

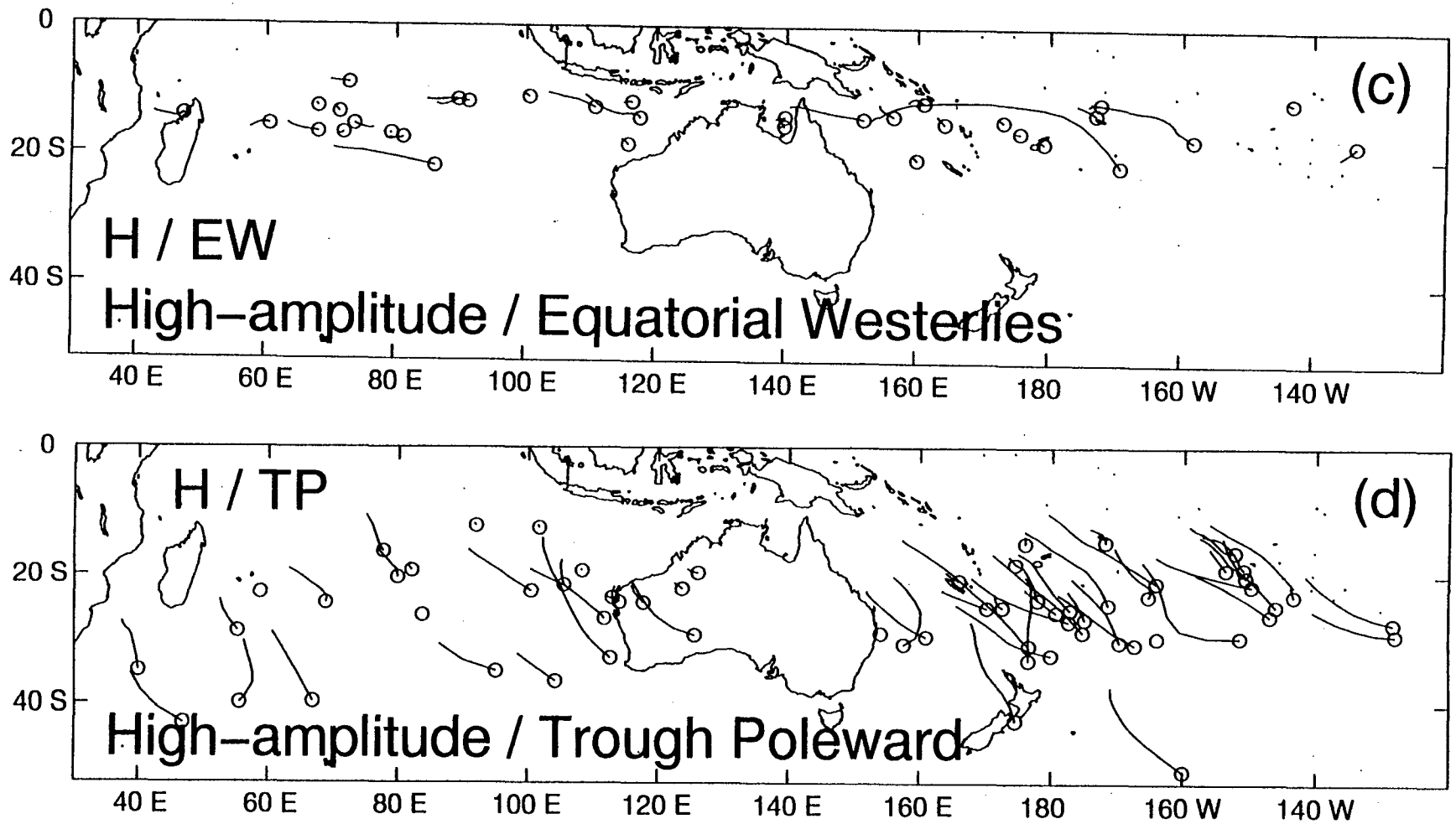

Fig. 7 (continued): Tracks in H synoptic pattern for the (c) Equatorial Westerlies (EW) and (d) Trough Poleward (TP) regions.

Whereas most of these tracks are short, which again reflects the transience of the H pattern, a few long tracks indicate the possibility of persistent conditions. The longest H/EW track in the South Pacific is that of TC Nina, which will be discussed in detail in Section 3c. This TC had a remarkable 30-kt translation owing to an interaction with TC Kina. During 1991-1998, the frequency of H/EW occurrences in the 12-h analysis was 4.9% and 3.7% in the South Pacific and South Indian Oceans, respectively. However, these statistics may be somewhat biased by the few long tracks in the South Pacific.

The 1991 – 98 sample has provided more examples of the rapid poleward motion in the Trough Poleward (TP) region of the H pattern (Fig. 2c). Although the many long southeastward tracks in the South Pacific Ocean are particularly evident in Fig. 7d, the sustained poleward motion under the influence of a meridional midlatitude trough also occurs frequently in the South Indian Ocean. As noted by Bannister et al. (1997), these TCs in H/TP account for a large fraction of the SH cases that are sustained to 30°S or beyond. Consequently, the vertical wind shear in these H/TP situations is smaller than might be expected in these latitudes. With the frequent occurrence and long H/TP tracks in the South Pacific, 14.3% of all 12-h analyses during 1991-98 were in this pattern/region. In the South Indian Ocean, the frequency was only 3.9%, but these anomalous tracks are difficult to forecast.

f. Multiple TC synoptic pattern

As indicated in Fig. 4, the Multiple (M) TC synoptic pattern (Fig. 2d) is rare in the SH. Only 0.4% and 0.9% of the South Indian Ocean cases are in the M/Equatorward Flow (EF) and M/Poleward Flow (PF) pattern/regions, respectively. Similarly, only 0.8% and 0.4% are in the M/EF and M/PF pattern/regions in the South Pacific. As indicated by Bannister *et al.* (1997), the relatively rare M synoptic patterns in the SH are because the number of multiple TCs with

separation distances of 10° - 20° lat. is small. In addition, the more transient and smaller amplitudes of the subtropical anticyclone cells in the SH does not allow establishment and maintenance of the pressure gradient implied by the conceptual model in Fig. 2d. An analogous synoptic situation with a TC in an enhanced pressure gradient between another TC and a high pressure cell will be defined in Section 3c. Although the M pattern does not occur frequently because of the need for a substantial subtropical anticyclone, semi-direct TC interactions do occur enough to warrant attention.

Even with an eight-year sample, only five cases of TCs in M/EF were found (Fig. 8a). Although important because equatorward displacements are not climatologically expected, the few cases and short tracks indicate the M/EF scenario is highly transient. Similarly, only four cases of M/PF were found during 1991-98 (Fig. 8b). These poleward tracks are anomalous because of the larger-than-expected translation speed in the region approaching the subtropical ridge. Rather than slowing down as in a recurvature scenario, these M/PF cases have an enhanced poleward environmental steering associated with the pressure gradient between the western TC and the eastern subtropical high pressure cell (Fig. 2d).

g. Environment structure transition summary

Since each synoptic pattern/region in Fig. 2 has a characteristic track direction and speed as in Figs. 5-8, the transition from one pattern/region to another will be accompanied by a track change. Thus, it is important for the forecaster to anticipate that such a transition will occur during the forecast interval. Transitional mechanisms that can lead to a change in environment structure are listed in Fig. 1. Many case studies with synoptic analyses and tracks associated with the more important transitions are given in Bannister *et al.* (1997). A new transition

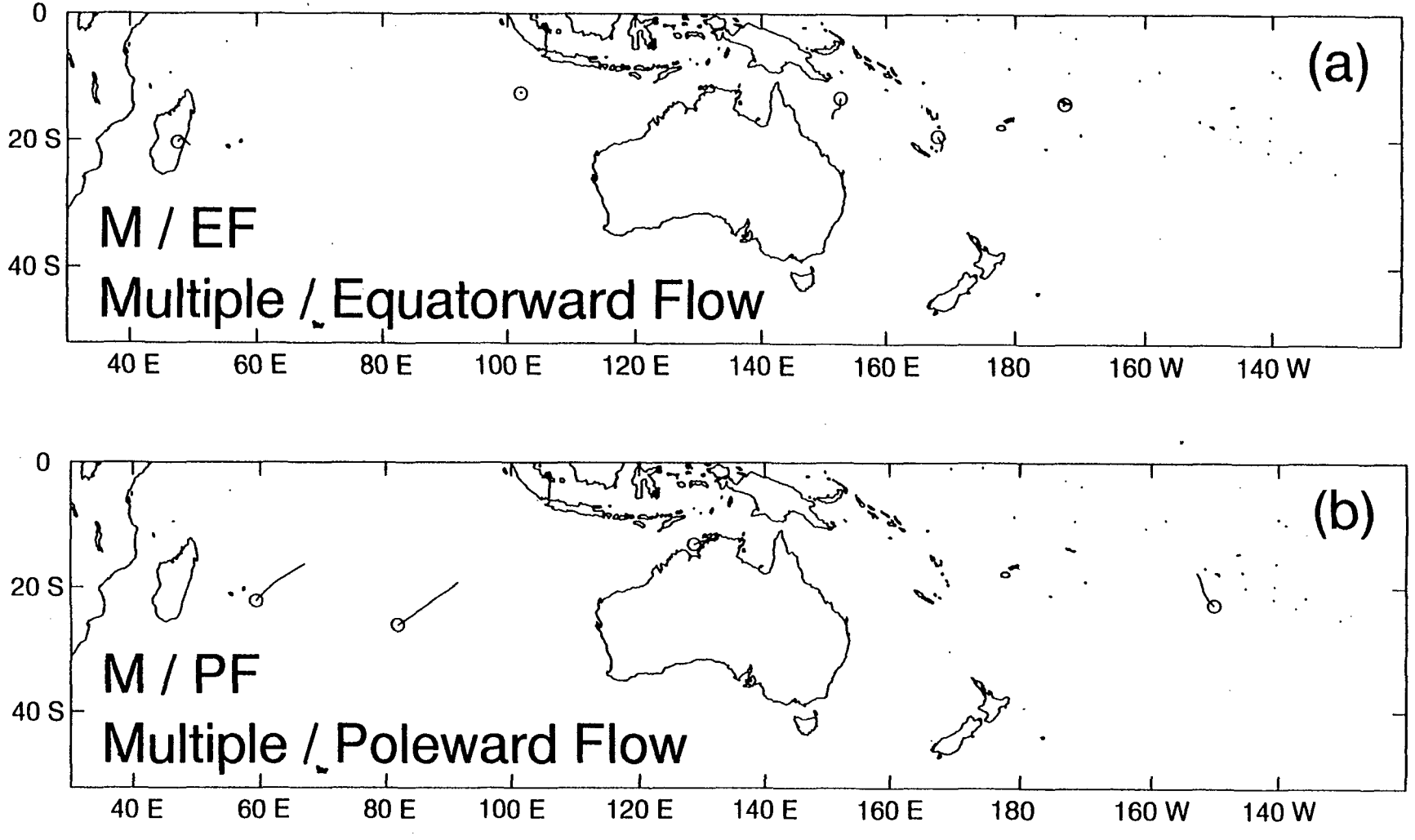

Fig. 8 Tracks as in Fig. 3, except only while the TCs are in the (a) M/Equatorward Flow (EF) and (b) M/Poleward Flow (PF) pattern/regions.

mechanism involving an Equatorial Westerly Wind Burst (EWWB) will be introduced with case studies in Section 3b.

The purpose of this section is to update the transition frequency summary given in Bannister *et al.* (1997) based on the expanded sample from 1991-1998. With the doubling of the data base, it is now possible to summarize with more confidence the South Indian Ocean (Fig. 9a) and the South Pacific Ocean (Fig. 9b) transitions than with the four-year sample.

With the eleven synoptic pattern/region combinations in the SH, many transitions are theoretically possible. In some cases three or fewer such transitions occurred during 1991-1998. Thus, only the "recurring" transitions (i.e., four or more cases) are included in Fig. 9. Whereas a total of 259 (165) transitions between pattern/regions was detected in the South Indian (Pacific) Ocean, only 203 (121) are defined as recurring in Fig. 9a (9b).

With the increase from 78 to 145 TCs in the South Indian Ocean data base (Fig. 9a), the number of recurring transitions (defined as > 2 in 1994-1997 sample) increased from 106 to 203 during 1991-1998. However, the two most frequent transitions are still the same: S/DR to P/PO and S/DR to S/WR with 35 and 23 transitions, respectively. Both of these transitions involve a turn from the most common westward S/DR track (Fig. 5b) in the South Indian Ocean to a more poleward track. Another frequent poleward track transition from the S/DR pattern/region is to the H/RP pattern/region. The next-most frequent transition from S/DR is to an eastward track in S/EW. Although this transition had been noted in the 1991-1994 sample, its recurrence in this sample led to the introduction of the EWWB transitional mechanism to be discussed in Section 3b.

In the South Indian Ocean (Fig. 9a), the S/DR pattern/region is also the most common "recipient" of a transition. Notice again the 21 transitions from S/EW to S/DR would involve a

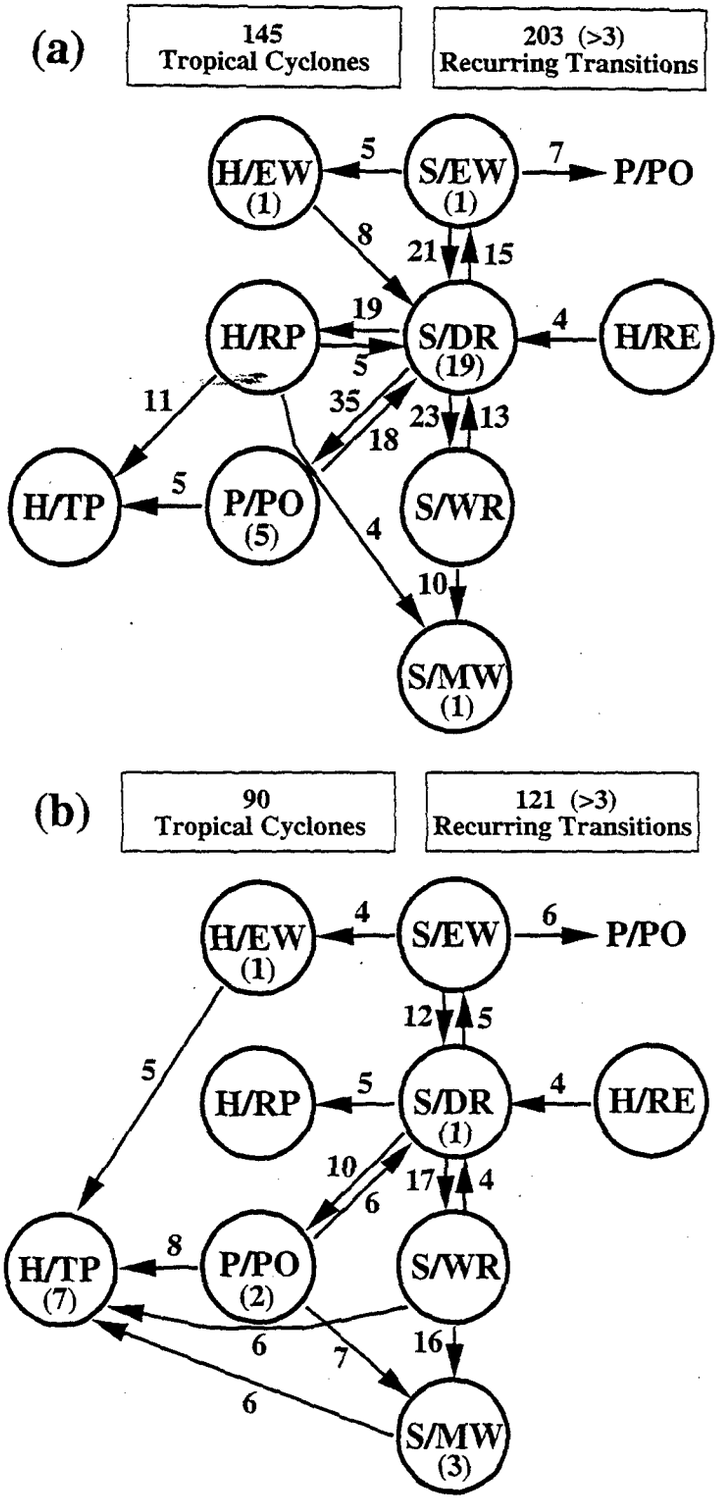

Fig. 9 Recurring (greater than three) environmental structure transitions for the (a) 145 TCs in the South Indian Ocean and (b) 90 TCs in the South Pacific Ocean during the 1990-1991 through 1997 – 1998 seasons.

track direction reversal, this time from eastward to westward. A relatively large number (18) of P/PO to S/DR transitions indicates a transient poleward track changing (back) to a westward track. Similarly, the "reverse transition" from a poleward S/WR track to a westward S/DR is a relatively large fraction of the S/DR to S/WR transitions in the South Indian Ocean. The westward-poleward-westward track sequence is sometimes called a "stairstep track," and is often associated with large forecast errors if the TC is forecast to recurve from S/WR into S/MW (10 transitions). Notice also the H/EW, H/RP, and H/RE with 8, 5, and 4 transitions to S/DR, respectively. These transitions imply a weakening of the meridional trough/ridge circulation of the H pattern such that the TC is then left equatorward of a (re-establishing) subtropical ridge. Finally, the H/TP tracks in the South Indian Ocean (Fig. 7d) originate in 11 cases from the H/RP (a recurvature through the subtropical ridge), or in 5 cases from the P/PO after the midlatitude trough became the primary poleward environmental steering.

The 1991-1998 sample of 90 TCs in the South Pacific Ocean (Fig. 9b) provided a much more comprehensive transition diagram than the 1991 – 1994 sample of 37 TCs in Bannister *et al.* (1997). The predominant transition path in the South Pacific is S/EW to S/DR to S/WR to S/MW with 12, 17, and 16 transitions, respectively. On a proportional basis, fewer of the first two of these transitions are followed by a reverse transition than occurs in the South Indian Ocean (Fig. 9a). For example, the ratio of S/DR to S/EW versus the opposite transition is 5/12 in the South Pacific versus 15/21 in the South Indian Ocean, and the ratio of S/WR to S/DR versus the opposite transition is 4/17 in the South Pacific versus 13/23 in the South Indian Ocean. These transitions suggest that South Pacific TCs in the S pattern may go through a more steady evolution with fewer track reversals than in the South Indian Ocean.

Another prominent feature of the South Pacific Ocean diagram (Fig. 9b) is the number of transitions to H/TP, which leads to the accelerating southeastward tracks in Fig. 7d. Notice that the transitions to H/TP originate from P/PO, S/WR, S/MW, and H/EW with 8, 6, 6, and 5 transitions, respectively. Whereas the H/EW to H/TP transition could be simply by advection (Fig.2c), the other three transitions suggest the approach of a vigorous midlatitude trough that "captures" TCs in these three already poleward tracks and accelerates that poleward motion.

Relative to the South Indian Ocean (Fig. 9a), the 10 S/DR to P/PO transition in the South Pacific Ocean is a smaller fraction of the 121 transitions (compared to 35 of 203). Another less frequent transition sequence in the South Pacific is from the H pattern/region combinations to the S/DR combinations. Although the rare H/RE cases do transition to S/DR, recurring transitions from H/EW and H/RP to S/DR that were noted in the South Indian Ocean (Fig. 9a) are absent in the South Pacific. This difference suggests the H pattern midlatitude troughs in the South Pacific do not relax back to a dominant subtropical ridge circulation as appears to be the case in the South Indian Ocean.

Just as the track diagrams in Figs. 5-8 illustrate differences in prevailing tracks between the South Indian and Pacific Oceans, the transition diagrams in Fig. 9 indicate different transition paths to and from these prevailing tracks. The forecaster should be aware of these differences in environmental structure changes.

3. Refinement of the Meteorological Knowledge Base

a. Background

The meteorological knowledge base of the Systematic and Integrated Approach to Tropical Cyclone (TC) Track Forecasting (hereafter the Systematic Approach) as applied to the Southern Hemisphere (SH) was described by Bannister *et al.* (1997). These concepts were based on Carr and Elsberry (1994), who described the roles of the environment structure and the TC characteristics in governing TC motion in the western North Pacific. The summary of these basic concepts as they apply in the SH are illustrated in Fig. 1. With the opportunity to double the SH cyclone database to eight years (Section 2) also came the opportunity to evaluate the set of TC-environmental conceptual models outlined in Bannister *et al.* (1997). This chapter summarizes some refinements from this evaluation.

Refinements that all pertain to the transitional mechanisms in the meteorological knowledge base are described in this section:

i) document additional transitional mechanisms and tropical cyclone interaction situations that were not noted in Bannister *et al.* (1997);

ii) reinforce the concept that the midlatitudes can play a vital role in determining TC motion in the SH via the Subtropical Ridge Modulation (SRM); and

iii) provide qualitative information to the forecaster on the vertical wind shear transitional mechanism.

b. Equatorial westerly wind burst transitional mechanism

(1) EWWB model description. In the adaptation of the Systematic Approach to the SH,

a new Equatorial Westerlies (EW) synoptic region of the Standard (S) pattern was introduced in Section 3 of Bannister *et al.* (1997). It was noted that a TC could form in the EW region and thus have an initial west-to-east track. It is also possible for a TC in the monsoon trough to transition into the EW region from the Dominant Ridge (DR) synoptic region. The EW region was also included in the High-amplitude (H) synoptic pattern to describe eastward TC motion in the region at the equatorward end of a deeply penetrating midlatitude trough.

A conceptual model of this Equatorial Westerly Wind Burst (EWWB) is shown in Fig. 10. Both the transition from the DR region to the EW region of the S pattern, and the continued eastward movement of some TCs, are often associated with a band of westerly winds along the equator. In the Before schematic, the TC is on the poleward side of the monsoon trough and thus is in the westward environmental steering of the S/DR pattern/region. The poleward shift or intensification of this equatorial band of anomalously strong winds on the equatorward side of the TC is occasionally sufficient to make it the dominant steering current for a TC (After schematic), rather than the easterly winds between the TC and the ridge (if any) on the poleward side of the TC. This scenario is often accompanied with a characteristic band of east-west oriented convection equatorward of the TC. Consequently, one of the clues that an EWWB scenario may be developing is enhanced cloudiness or cloud organization equatorward of the TC.

(2) EWWB model illustrations. The first of three EWWB examples is shown in Fig. 11. At 12 UTC 6 December 1991, the western cyclone (TC Val) is moving to the southeast in the S/EW pattern/region, while the eastern cyclone (TC Wasa) is drifting to the south-southwest in the S/WR pattern/region. In conjunction with the EWWB event that will affect TE Wasa, both TCs will then track eastward.

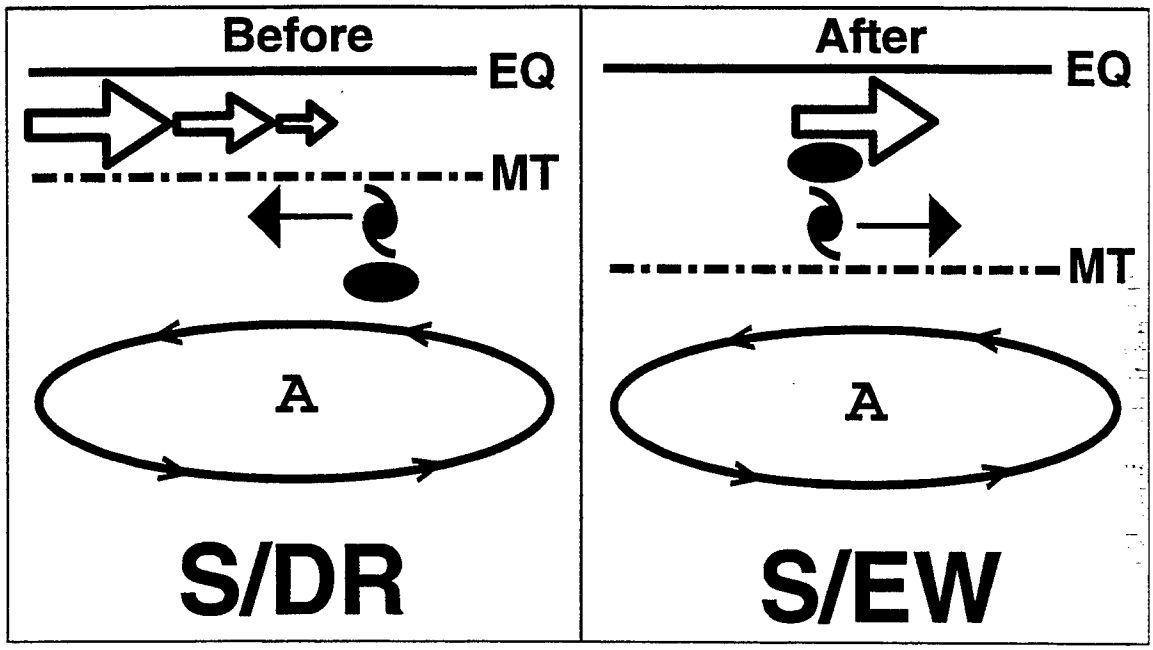

Fig. 10 Conceptual model of Equatorial Westerly Wind Burst (EWWB) transitional mechanism. The symbols EQ, MT, and A are for Equator, Monsoon Trough, and subtropical Anticyclone. The open arrows indicate the approach of an Equatorial Westerlies wind burst to the equatorward side of the TC, which subsequently changes the direction of motion (thin arrow).

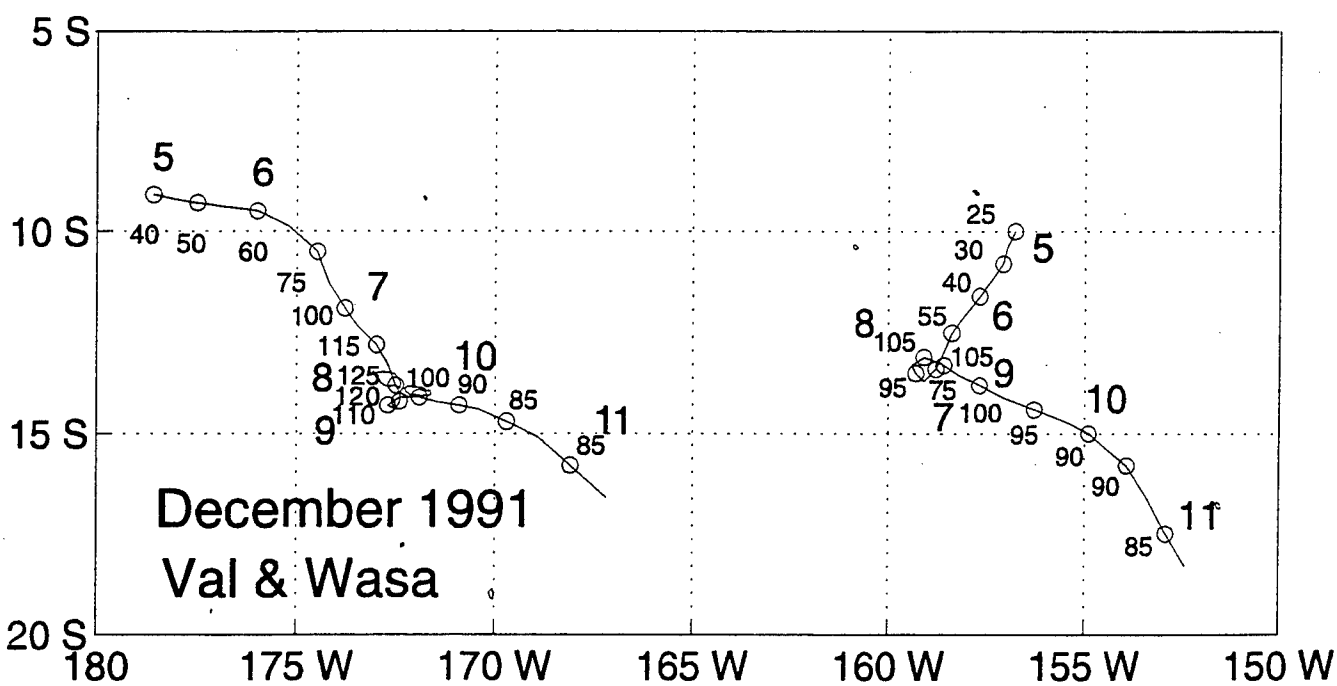

Fig. 11 Best tracks of the western TC Val (0692) and the eastern TC Wasa (0792) during 00 UTC 5 December to 00 UTC 11 December 1991. TC positions are indicated each 12 h (circles) with the date (large numeral) adjacent to the 00 UTC position and the intensity (kt; small numerals).

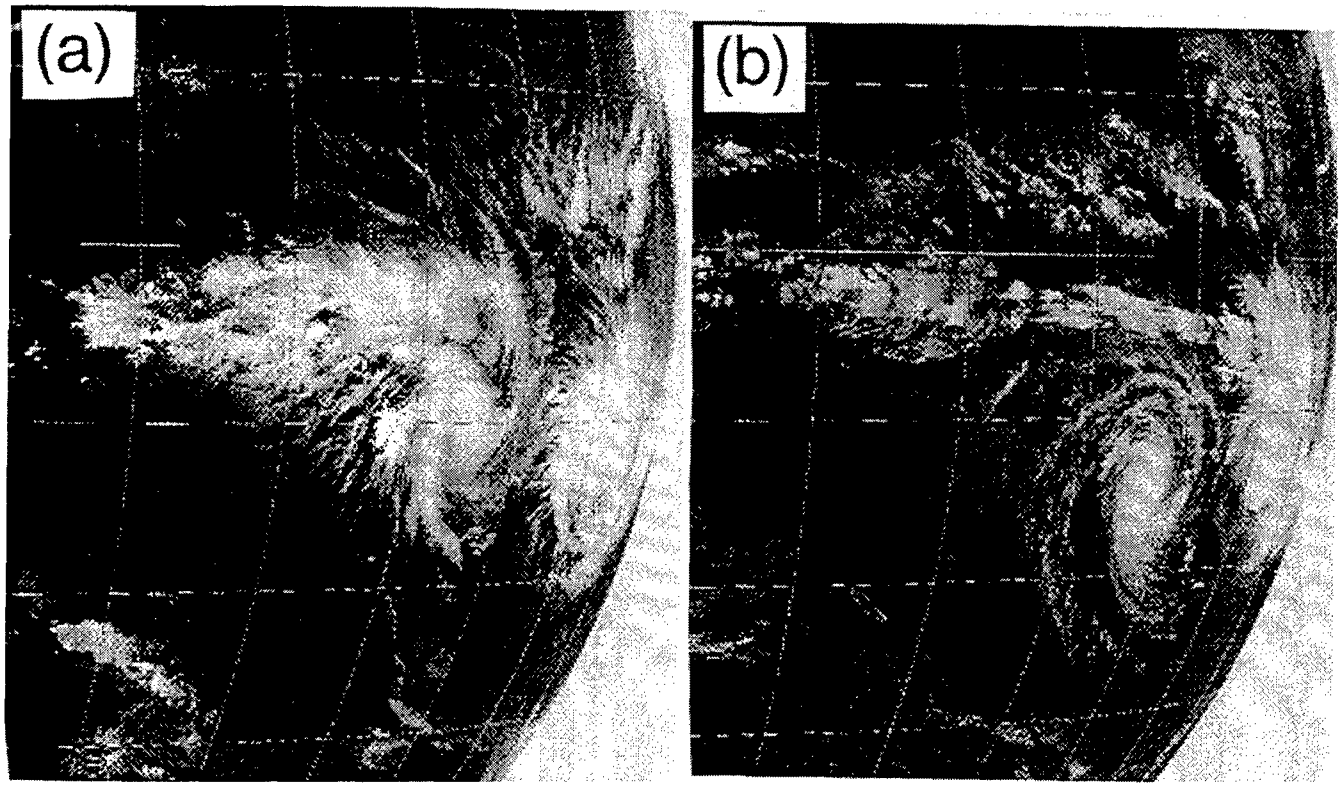

Fig. 12 Geostationary Meteorological Satellite infrared imagery at (a) 03 UTC 6 December and (b) 03 UTC 9 December 1991.

Inspection of the IR satellite imagery in Fig. 12a indicates a broad, east-west band of deep convection to the north and northwest of TC Val, which is consistent with a band of Equatorial Westerlies that is advecting Val towards the southeast. However, this cloud band does not extend east of Val so that a clear break exists between that cloud band and TC Wasa. The NOGAPS 500-mb analysis valid for 12 UTC 6 December 1991 (Fig. 13a) does have an isotach maximum to the north and northeast of TC Val, which is expected for the southeastward motion. Since westerlies are evident at 500 mb to the northwest of Val, the equatorial cloud band has deep westerlies from the surface to at least 500 mb. The slow southwestward drift of TC Wasa is evidently a reflection of slightly stronger environmental steering associated with a weak ridge to the south, rather than the northwesterlies to the north that are indicated by the

small 20-kt isotach maximum. Thus, TC Wasa is still in the S/WR pattern/region as the extension of the monsoon cloud band and stronger Equatorial Westerlies have not sufficiently affected its environmental steering.

The situation changes by 00 UTC 9 December 1991, when both TC Val and TC Wasa are moving eastward (Fig. 11). The IR satellite imagery (Fig. 12b) now indicates the equatorial cloud band has extended eastward to the north of both cyclones. The NOGAPS 500 mb analysis (Fig. 13b) also has a large and strong isotach maxima to the north of both cyclones, which indicates the associated Equatorial Westerlies have become the environmental steering for both cyclones. The change to eastward tracks indicates the transition to the S/EW pattern/region (Fig. 2a) via the EWWB transitional mechanism is completed.

The satellite imagery and NOGAPS analysis in the above example are in good agreement. However, the operational cyclone forecaster must be aware that other situations are not so clear. The second example indicates that satellite interpretation can be crucial in the recognition of the EWWB. At 00 UTC 13 November 1991 (Fig. 14a), the pre-TC Tia disturbance is slowly moving to the southwest equatorward of a col in the mid-tropospheric subtropical ridge axis. Notice the loose organization of the clouds to the north of the disturbance in the satellite image (Fig. 14b).

By 00 UTC 14 November 1991, TC Tia had turned sharply towards the east. No changes in the circulations in the 500-mb (or other level) NOGAPS analyses (Fig. 15a) are evident that would explain this track change. However, inspection of the IR satellite imagery at the same time (Fig. 15b) indicates that an EWWB is in process to the north of the TC. Notice that the linear east-west cloud feature is significantly enhanced from that of 24 h previously (Fig. 14b). This example illustrates that the objective analyses in the SH are sometimes inadequate to

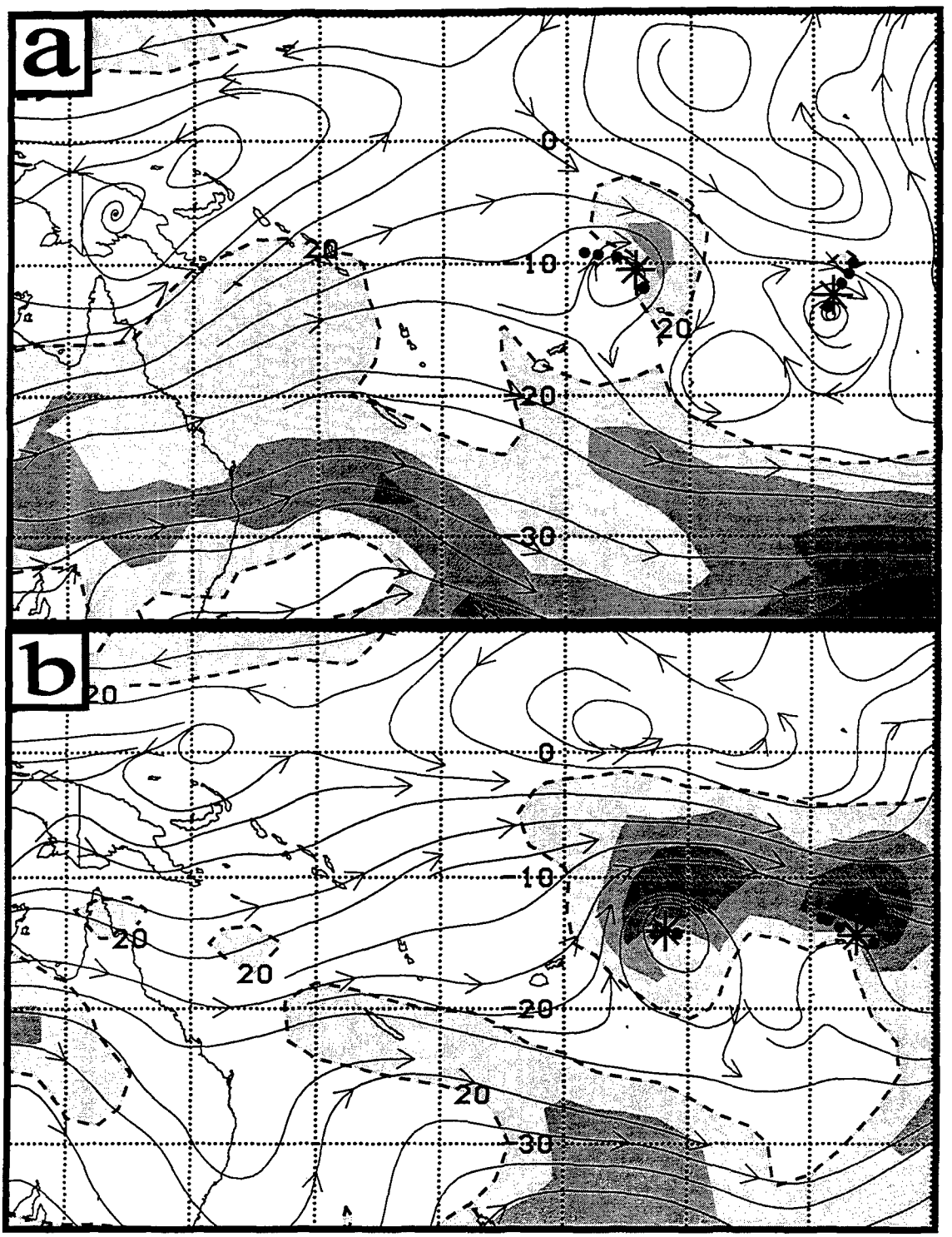

Fig. 13 NOGAPS 500-mb analysis valid at (a) 12 UTC 6 December 1991 and (b) 00 UTC 9 December. Streamlines are thin solid lines and isotachs (kt) are dashed for 20 kt and then shaded progressively darker for each 10 kt interval. The present storm position is indicated by an asterisk and the –36, -24, -12, and +12 h positions are indicated by dots. The western (eastern) TC is Val (Wasa).

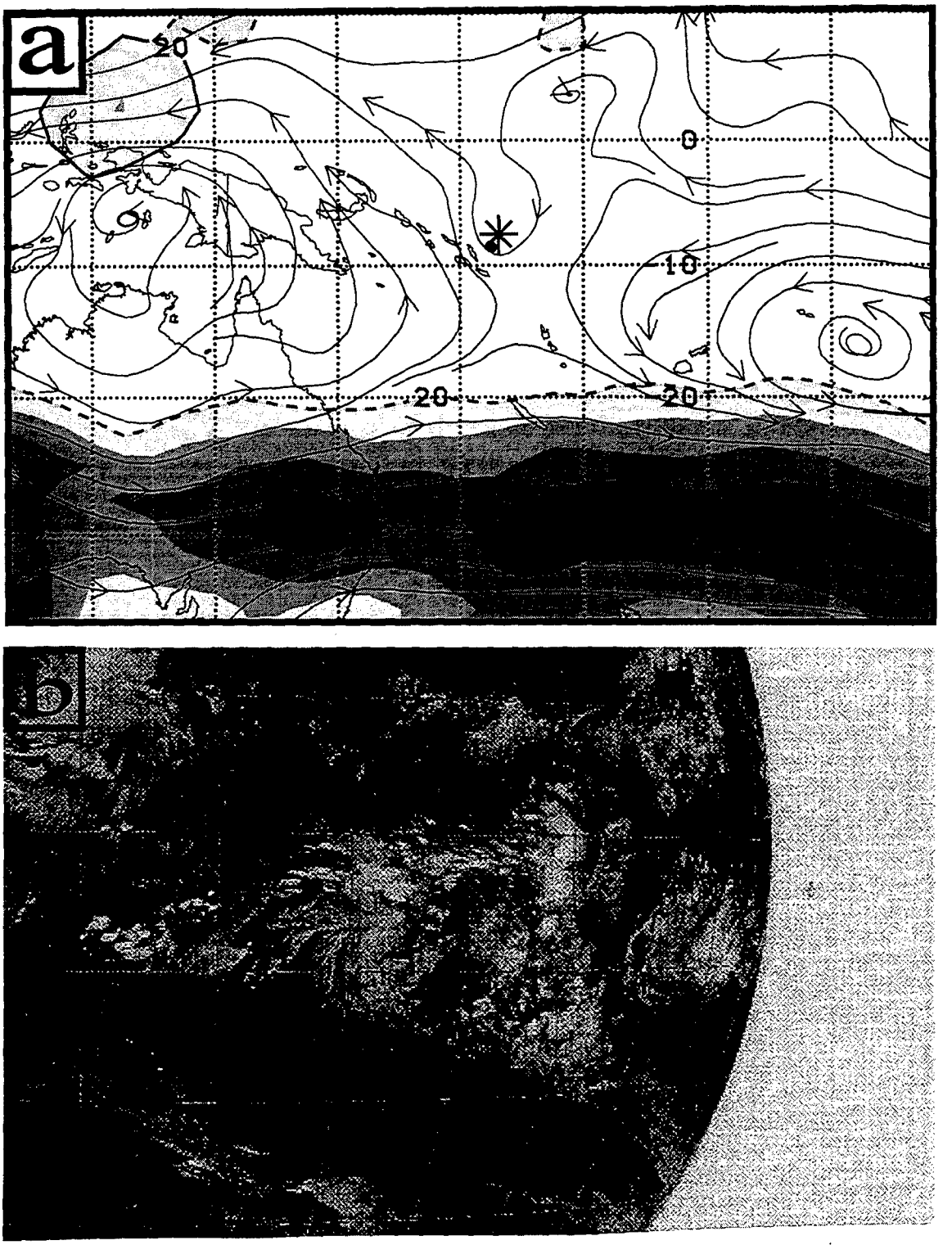

Fig. 14 (a) NOGAPS 500-mb analysis as in Fig. 13, except valid at 00 UTC 13 November 1991, and (b) the GMS IR imagery at 03 UTC 13 November 1991. The pre-TC Tia disturbance is near the center of the satellite image.

explain the TC motion, probably due to data sparsity. However, careful analysis of the satellite imagery to detect the presence of the EWWB transitional mechanism can explain the apparently baffling eastward movement of TC Tia.

In the third EWWB illustration, TC Lena had a dramatic change in track during 29-31 January 1993 (Fig. 16). This track change has been associated with a rather subtle change in environmental steering.

At 12 UTC 27 January 1993 (Fig. 17a), TC Lena is tracking to the west on the equatorward side of a zonal mid-tropospheric ridge. A possible complicating factor is that TC 14P to the east of TC Lena is also tracking to the west. Both cyclones are in the S/DR pattern/region (Fig. 2a) with a well-defined isotach maximum on the poleward side of TC Lena.

At 12 UTC 28 January (Fig. 17b), TC Lena is still tracking westward. However, the 20-kt isotach poleward of Lena has reduced in size, while the 20-kt isotach on the equatorward side of TC Lena has increased in areal extent and moved closer. Although the forecaster would not have knowledge of the +12 h position in Fig. 17b, it indicates that Lena is about to slow down. Large changes in the synoptic pattern are evident by 12 UTC 29 January (Fig. 17c). The subtropical ridge to the south of Lena is being weakened by an amplifying trough to the southwest. Whereas the 20-kt isotach equatorward of Lena has not moved closer to Lena, the 20-kt isotach to the south has continued to reduce in size. TC Lena has stopped moving westward during this period, which should alert the forecaster to search for changes in the environmental steering (assuming that this center fix has been checked and found to be accurate). The possibility of an Semi-direct TC Interaction (STI) with TC 14P to the east should also be examined, owing to the poleward turn of that TC (Bannister *et al.* 1997, Fig. 5). However, the separation between the

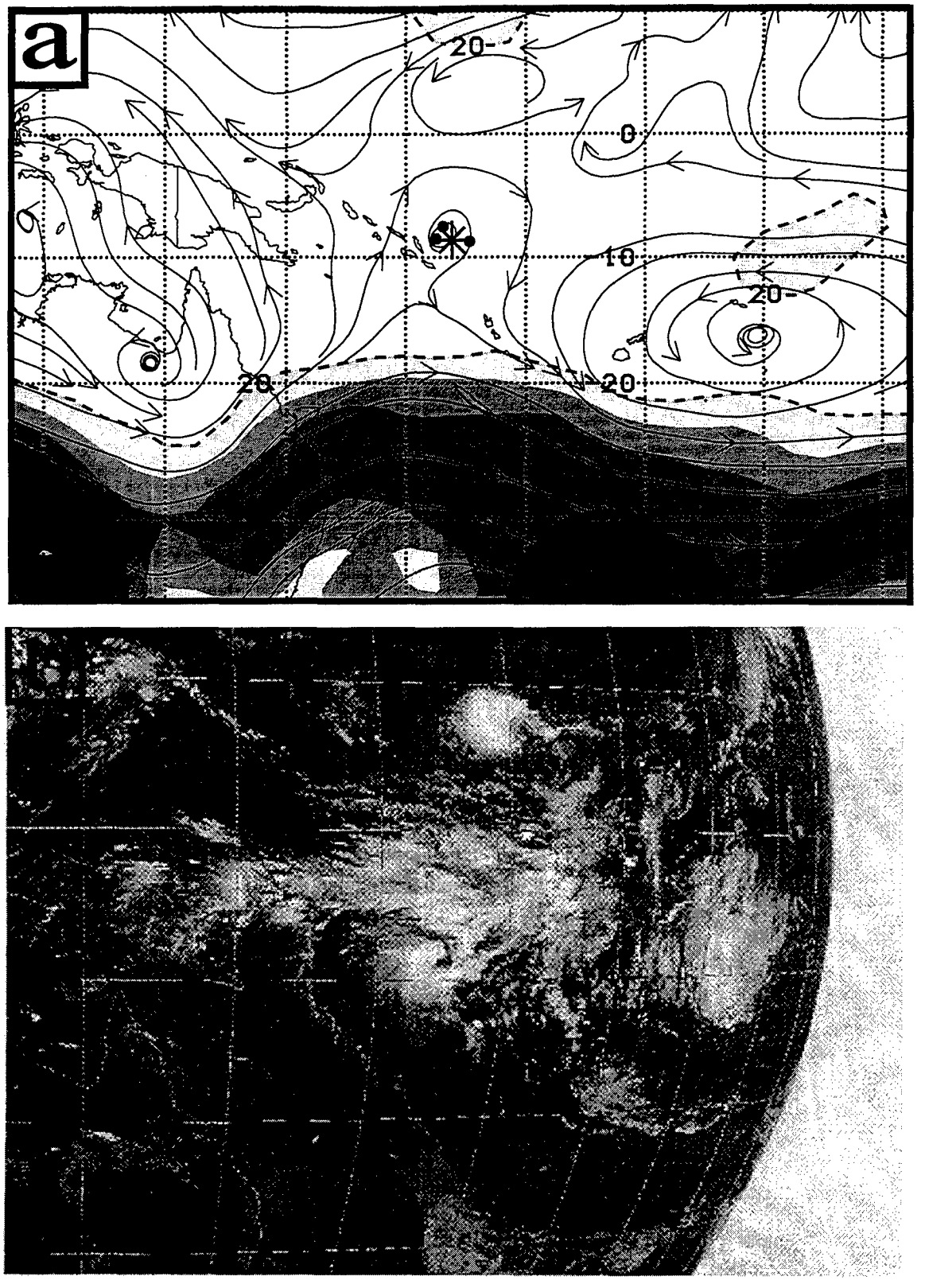

Fig. 15 (a) NOGAPS 500-mb analysis as in Fig. 13, except at 00 UTC 14 November 1991, and the (b) GMS IR imagery at 03 UTC 14 November 1991.

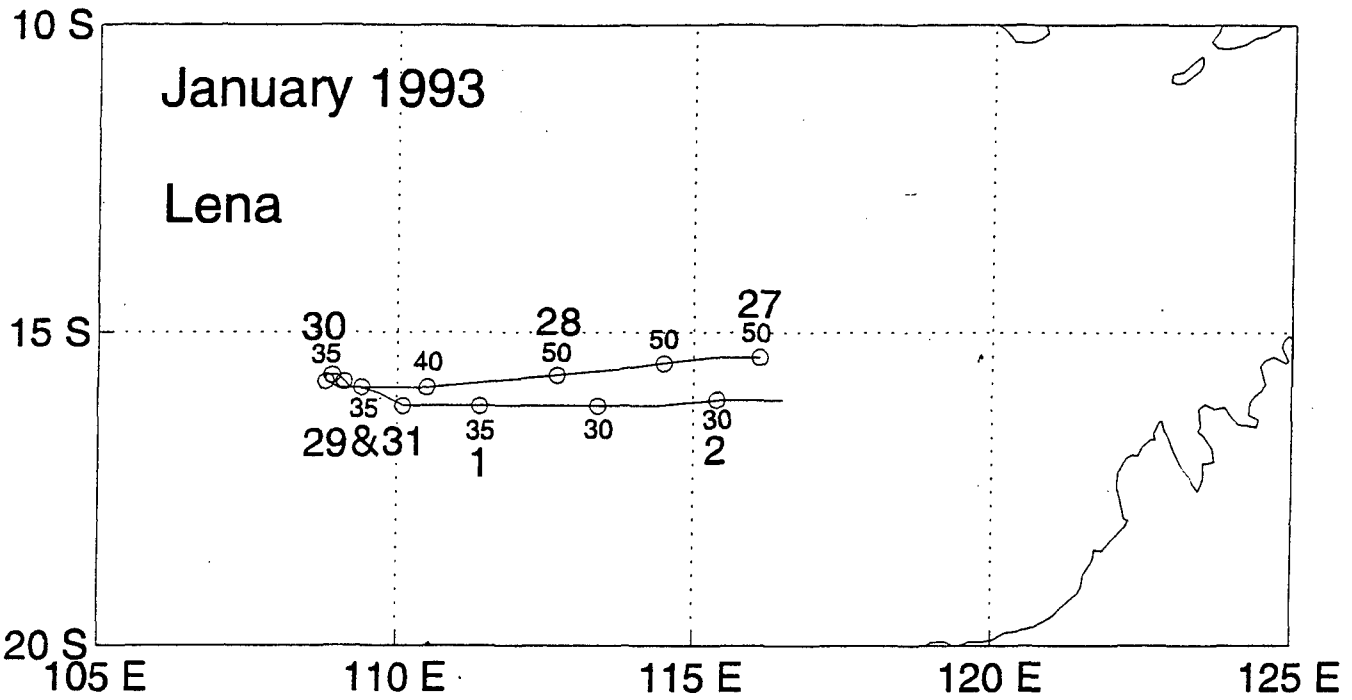

Fig. 16 Best track as in Fig. 11, except for TC Lena (1393) between 00 UTC 27 January 1993 and 00 UTC 2 February.

two TCs is rather large, and TC Lena has simply stopped, rather than turning equatorward as in the STI conceptual model.

By 00 UTC 31 January (Fig. 17d), TC Lena has begun to track east-southeastward. The environmental steering is indicated by the 20-kt isotach that is associated with well-established Equatorial Westerlies to the north of Lena. To the south, the subtropical ridge has been almost completely replaced by the midlatitude trough that had been advancing from the west. However, the trough amplitude is not sufficiently large to become the environmental steering of TC Lena, which would be designated as a H pattern. Given the change to an eastward track, TC Lena has now completed a S/DR to S/EW transition via the EWWB transitional mechanism.

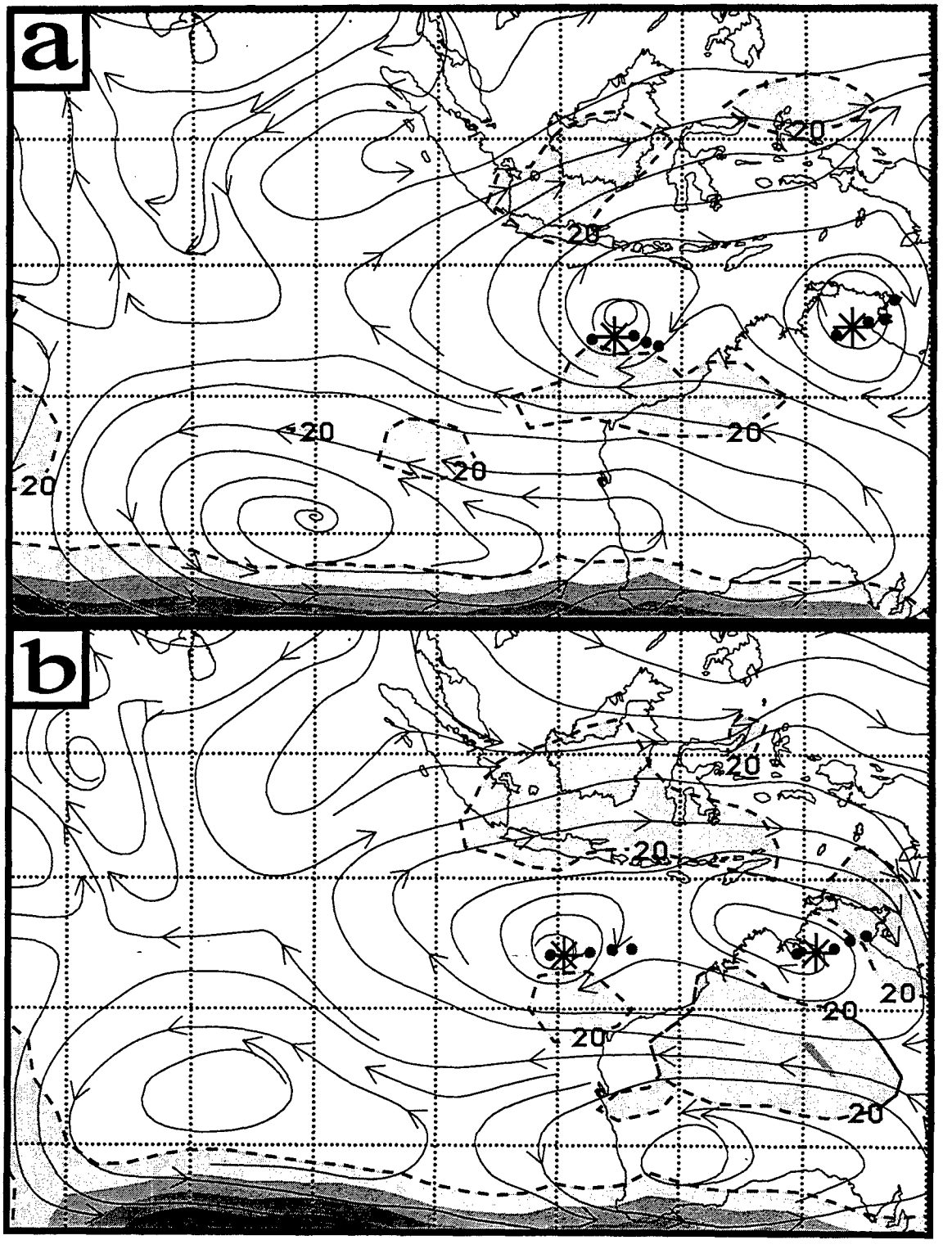

Fig. 17 (a) NOGAPS 500-mb analysis as in Fig. 13, except valid at 12 UTC 27 January, (b) 28 January, (c) 29 January, and (d) 00 UTC 31 January 1993.

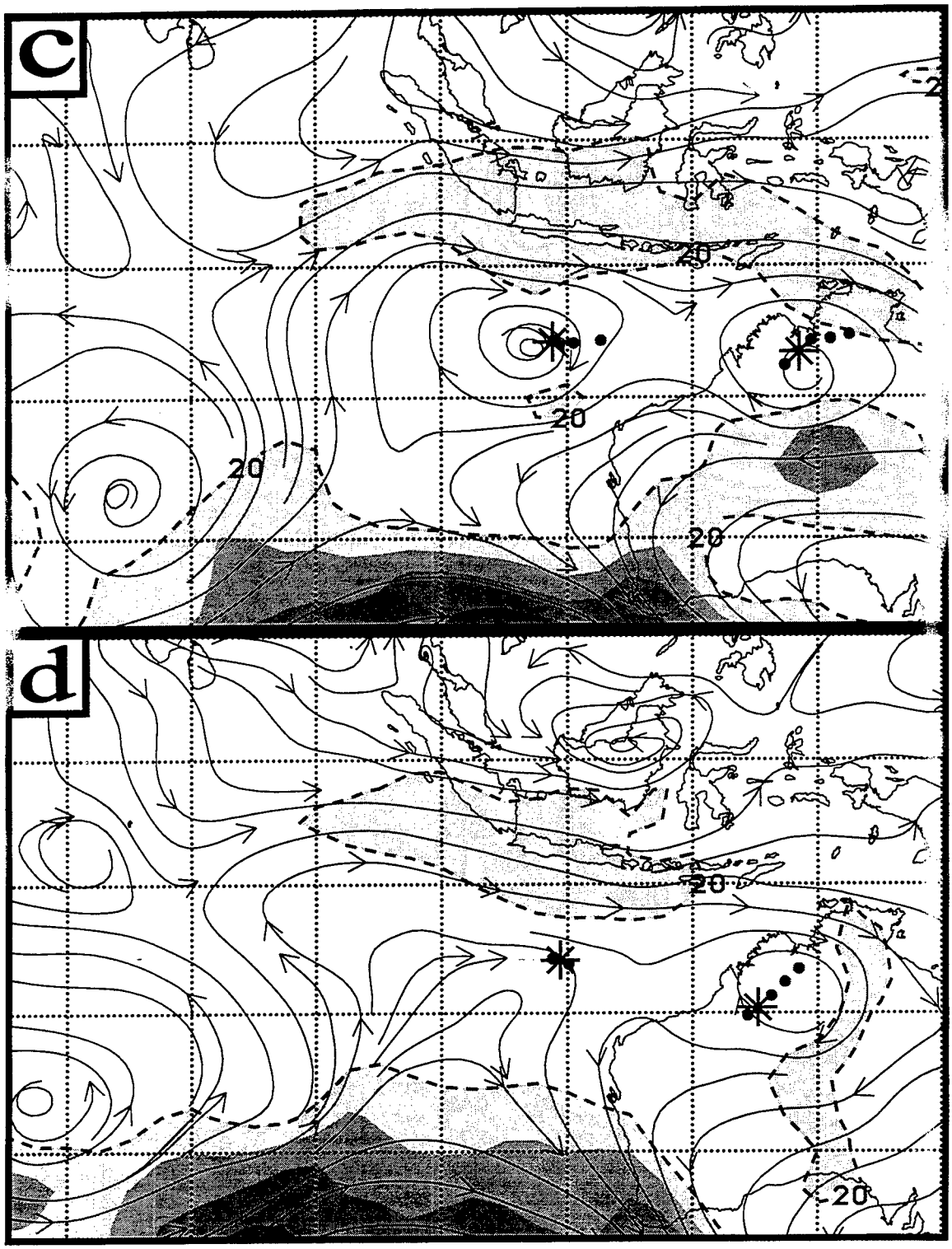

Fig. 17 (continued) (c) NOGAPS 500-mb analysis valid 12 UTC 29 January and 00 UTC 31 January 1993.

During this period, a pre-existing Equatorial Westerlies region expanded poleward and intensified as in the conceptual model in Fig. 10. At the same time, the ridge to the south of the TC was being eroded in response to an approaching midlatitude trough from the west. This example reinforces the importance of assessing competing steering regimes in all quadrants of a TC. Clearly, the forecaster must be aware of the presence of a vigorous monsoon trough and alert to the possibility that the associated Equatorial Westerlies on the equatorward side may affect the environmental steering of a TC.

The question that may be asked in this example is what would have happened if there had not been an advancing midlatitude trough from the southwest? Would the EWWB acting alone have changed the track of Lena, i.e., would the S/EW steering current induced by the EWWB have been enough to overcome the S/DR steering current associated with the zonal ridge poleward of the TC? The answer depends on which steering current is stronger and impinges more on the TC, which can be a very difficult forecast problem. It is not clear from this sequence of analyses whether the environmental steering and track changes would have occurred if the subtropical ridge had not been weakened. In this case, the forecaster needed to realize late on 28 January leading into 29 January that the S/DR and S/EW steering currents were tending to offset, and that the TC was beginning to slow down. The ability of the numerical models to forecast such a subtle shift in environmental steering needs to be assessed. If the numerical model forecast indicated that the midlatitude trough to the southwest would continue to progress eastward and that the Equatorial Westerlies would persist, he/she would have a basis to forecast a major change in track direction from what would have been expected from a persistence-type westward track equatorward of the subtropical ridge.

If the midlatitude trough was strong enough to break the subtropical ridge, another alternative is that the TC might move into the S/WR pattern/region in advance of this trough, and perhaps even recurve into the midlatitude westerlies. Too much attention to the midlatitude evolution without considering also the intensifying Equatorial Westerlies could have again led to a wrong track forecast scenario.

c. Tropical cyclone interaction-related refinements

(1) Semi-direct tropical cyclone interaction equatorward (STIQ) and poleward (STIP) conceptual model. Binary TC interactions as defined by Carr et al. (1997) and adapted for the SH were described in Bannister *et al.* (1997) Section 2e. Semi-direct TC Interactions (STI) were classified as STIE or STIW depending on which TC (eastern or western) was being affected. This scenario may also be described as being a Multiple (M) TC synoptic pattern (Fig. 2d). For this type of STI interaction, the two TCs must be separated by more than 10° lat., oriented approximately east-west, and be within about 10° lat. of the subtropical ridge axis. The environmental steering of the western (eastern) TC is equatorward (poleward) because of the pressure gradient between the eastern (western) TC and the subtropical high pressure cell to the west (east).

In the new sample when two or more cyclones were present at low latitudes in a SH basin, it was observed that a northern TC between the equatorial buffer cell and another TC to its south or southeast would have an enhanced eastward motion. The conceptual model for Semi-direct TC Interaction Equatorward (STIQ) is given in Fig.18. Analogous to the STI scenario, the eastward environmental steering current appeared to be enhanced by the increased pressure gradient between the high pressure in the equatorial buffer cell and the low pressure in the

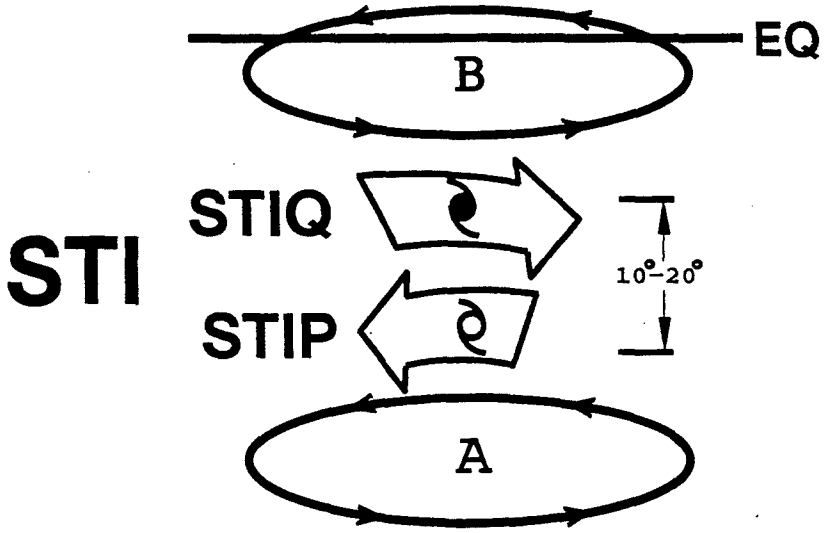

Fig. 18 Conceptual model, as in Fig. 10, except for the Semi-direct TC Interaction (STI) involving the equatorward TC (STIQ) with the equatorial Buffer (B) cell, or involving the poleward TC (STIP) with the subtropical Anticyclone (A).

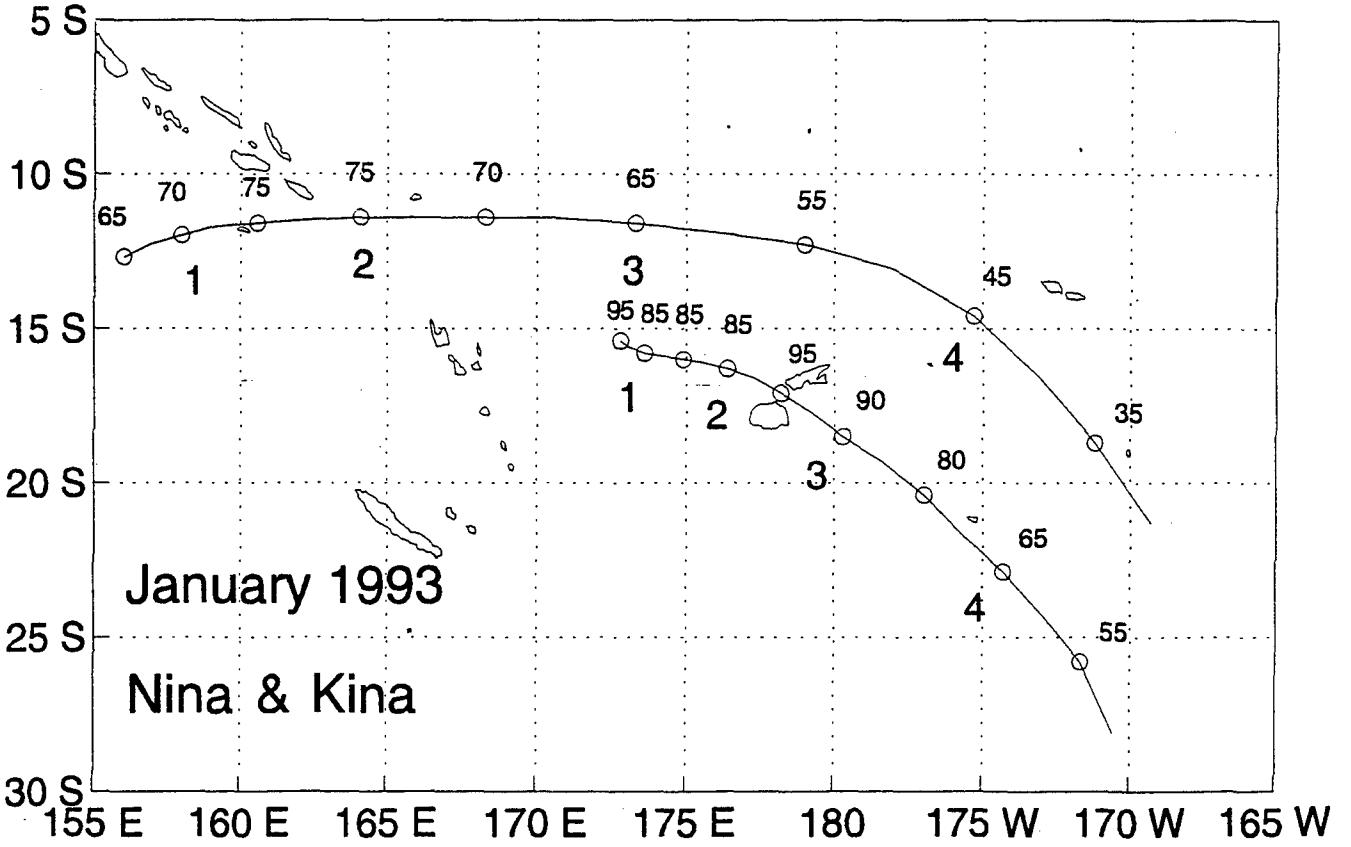

Fig. 19 Best tracks as in Fig. 11, except for the equatorward TC Nina (0693) and the poleward TC Kina (0793) during 12 UTC 31 December 1992 to 12 UTC 4 January 1993.

poleward TC. This increase in the eastward environmental steering across the equatorward TC is defined as STIQ.

Although no cyclone has yet been labeled as such, it is conceivable that the poleward TC may be in an enhanced pressure gradient between the high pressure in the subtropical ridge and the low pressure in the equatorward TC. Such an increase in the westward environmental steering across the poleward TC would be called Semi-direct TC Interaction Poleward (STIP), and this possibility is indicated in Fig. 18.

(2) STIQ model illustration. From 12 UTC 1 January 1993 to 12 UTC 3 January 1993, the TC Nina translation speed increased from 15 kt to a remarkable 30 kt while moving generally eastward along 12°S (Fig. 19). During the same time period, TC Kina (0793) was to the southeast of Nina and moving eastward at a slower speed.

The NOGAPS 500-mb analysis for 12 UTC 1 January (Fig. 20a) indicates that the two TCs were in an eastward stream between the equatorial buffer cell and the equatorward end of a broad midlatitude trough that had penetrated deep into the tropics. Thus, both TCs are classified in the H/EW pattern/region (Fig. 2c). By 12 UTC 2 January (Fig. 20b), the Equatorial Westerlies to the north of the TCs had increased in areal extent and in intensity (notice increased isotach maxima). Very rapid eastward translation is evident from the TC Nina positions plotted on the NOGAPS analysis at 12 UTC 3 January 1993 (Fig. 20c). The translation speed increase of Nina during 12 UTC 2 January to 12 UTC 3 January results from the superposition of the eastward steering flow on the equatorward side of Kina and the eastward steering flow associated with the EWWB. Consequently, the accelerated translation is consistent with the STIQ conceptual model in Fig. 18. Meanwhile, TC Kina has also increased in translation speed and turned poleward in

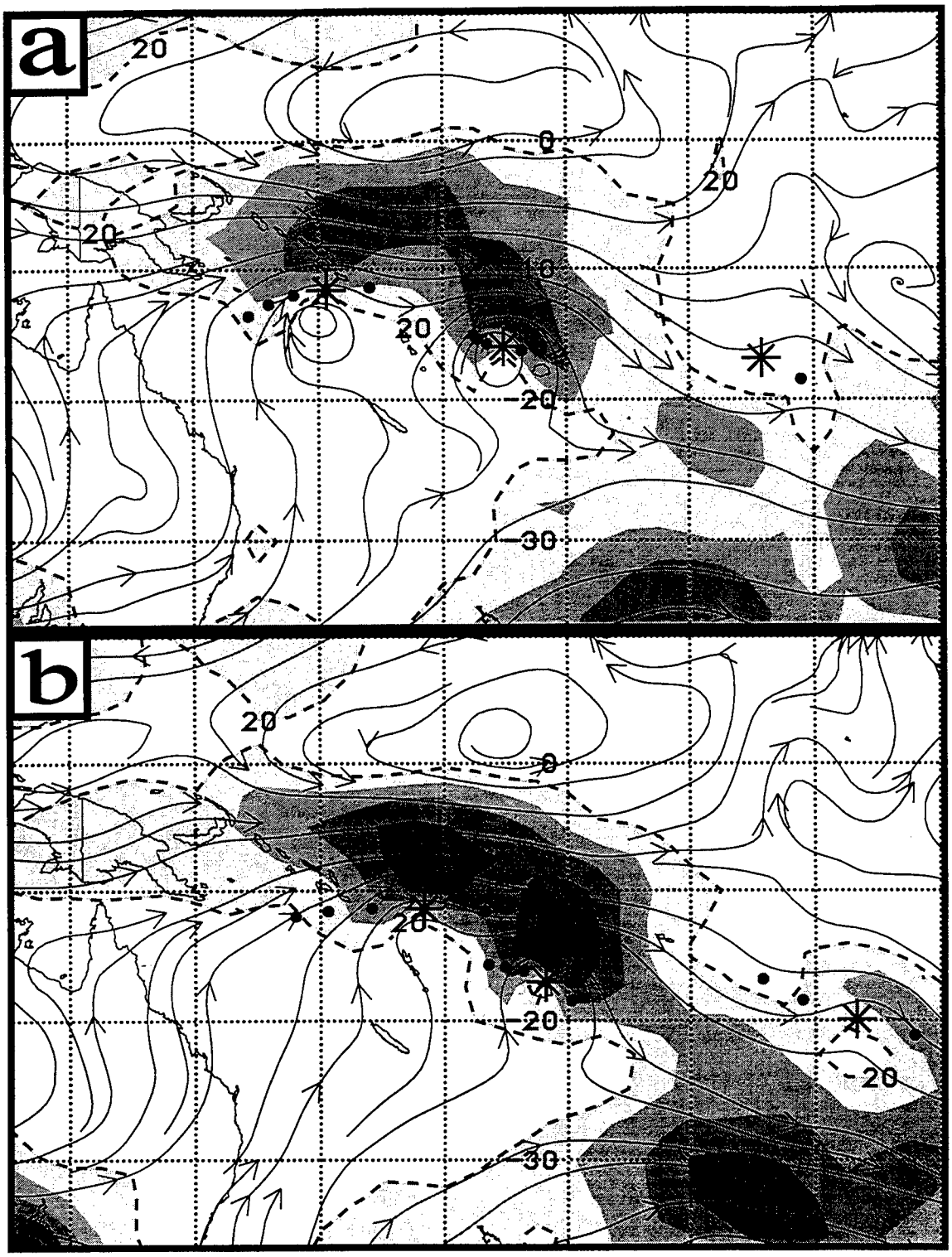

Fig. 20 NOGAPS 500-mb analyses as in Fig. 13, except valid at 12 UTC (a) 1 January, (b) 2 January, and (c) 3 January 1993.

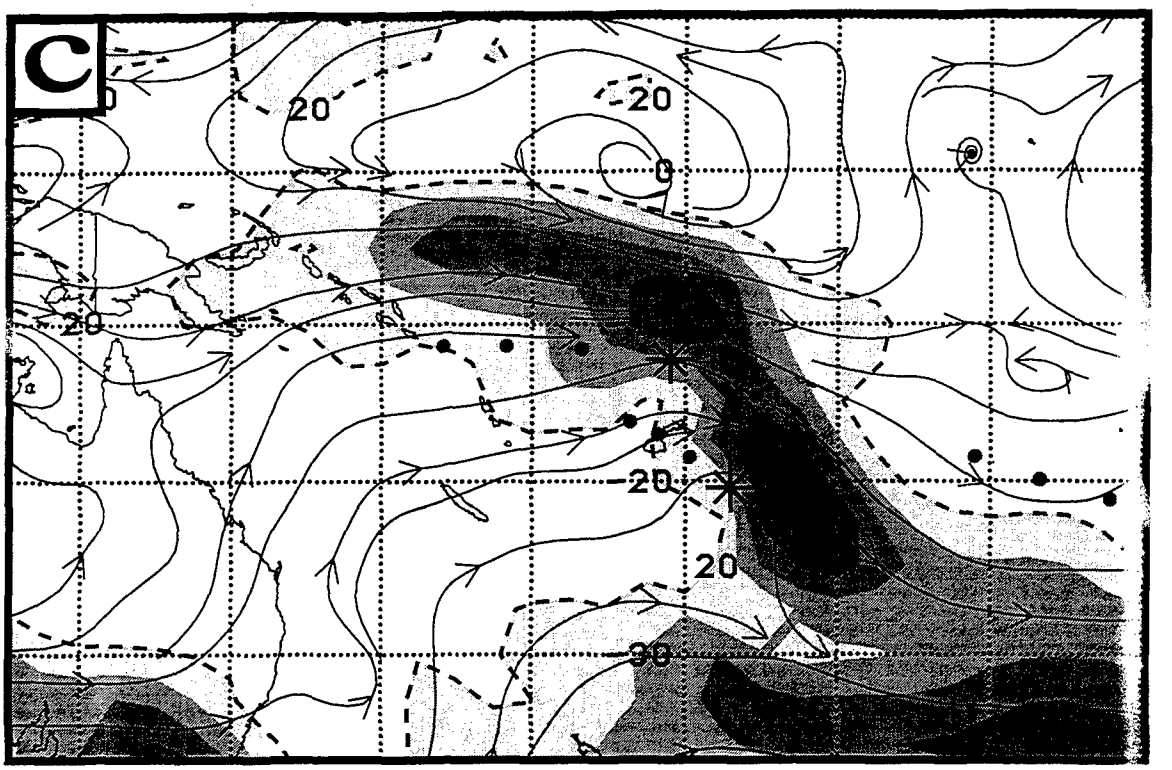

Fig. 20 continued (panel c).

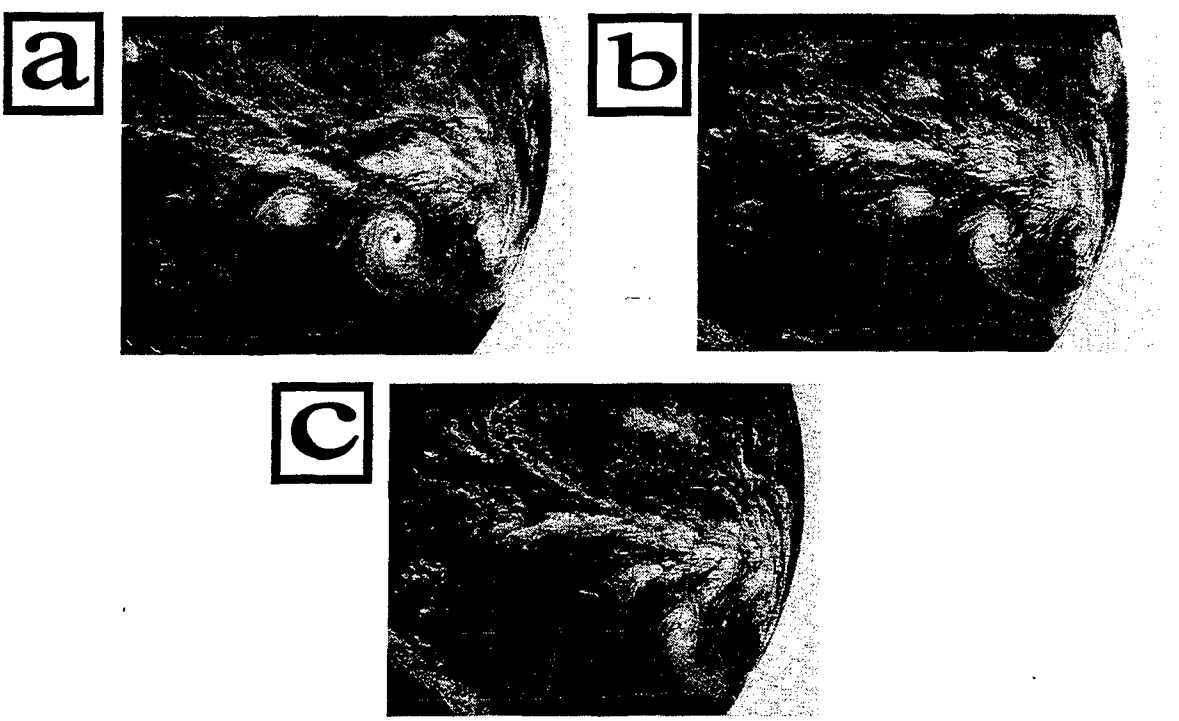

Fig. 21 GMS IR imagery 03 UTC on (a) 1 January, (b) 2 January, and (c) 3 January 1993.

response to an approaching midlatitude trough. Given this track direction and rapid translation speed, TC Kina would be classified in the H/TP pattern/region (Fig. 2c).

Satellite imagery during this period (Fig. 21) indicates a period of EWWB. At the initial time (Fig. 21a), the equatorial cloud band appears to be best organized north of TC Nina, and less concentrated to the north of TC Kina. Although a break existed between the two cloud bands at the initial time, 24 h later (Fig. 21b) a continuous, concentrated cloud band extends east-west equatorward of the two TCs. Notice that Nina has now moved eastward into a potentially favorable alignment for STIQ (Fig. 18) with Kina to the southeast and the equatorial buffer cell to the northwest. Whereas the extensive cloud band is still present 24 h later and Nina is still in a favorable alignment for STIQ (Fig. 21c), TC Nina has decreased in intensity and TC Kina has turned poleward and is also decreasing in intensity. Thus, the large translation speed of Kina may be attributed to this EWWB event as well as the STIQ transitional mechanism.

d. Subtropical ridge modulation (SRM) refinements

Many of the case studies in Bannister *et al.* (1997) included a mention of the SRM transitional mechanism. Generally, these examples of SRM involved the juxtaposition of a midlatitude trough (SRMT) or ridge (SRMR) with the subtropical ridge as the process to effect a change in the track of a TC. While these modes of SRM are analogous to those originally developed for the western North Pacific, the weaker subtropical anticyclone in the SH is highly transient and frequently disrupted by midlatitude trough/ridge systems. Indeed, the midlatitude westerlies and the subtropical anticyclone in the SH may be considered to be dynamically more linked as troughs intrude equatorward and ridges push poleward. It is important for the forecaster to recognize both the midlatitude intrusions that modify the subtropical ridge and that

the weakening of a deeply penetrating midlatitude trough (defacto SRMR) or a weakening of a pre-existing midlatitude ridge (defacto SRMT) may also affect the TC track.

(1) SRM weakening. This case study is of a midlatitude trough that is presently affecting the track of TC Alexandra, and the change of the TC track as that trough weakens. The track of TC Alexandra during 20 December to 26 December 1991 is shown in Fig. 22. A dramatic change in the track occurs from being toward the southeast during 21 and 22 December to a westward track by 24 December. The first NOGAPS 500-mb analysis (Fig. 23a) indicates that TC Alexandra is in the TP region of a High-amplitude pattern with a trough to the west that has penetrated all the way to the Equator. Notice the major cutoff low just to the west of Australia and the narrow intervening ridge between this cutoff and the trough associated with Alexandra. Twenty-four hours later (Fig. 23b), the western trough weakens while it continues to

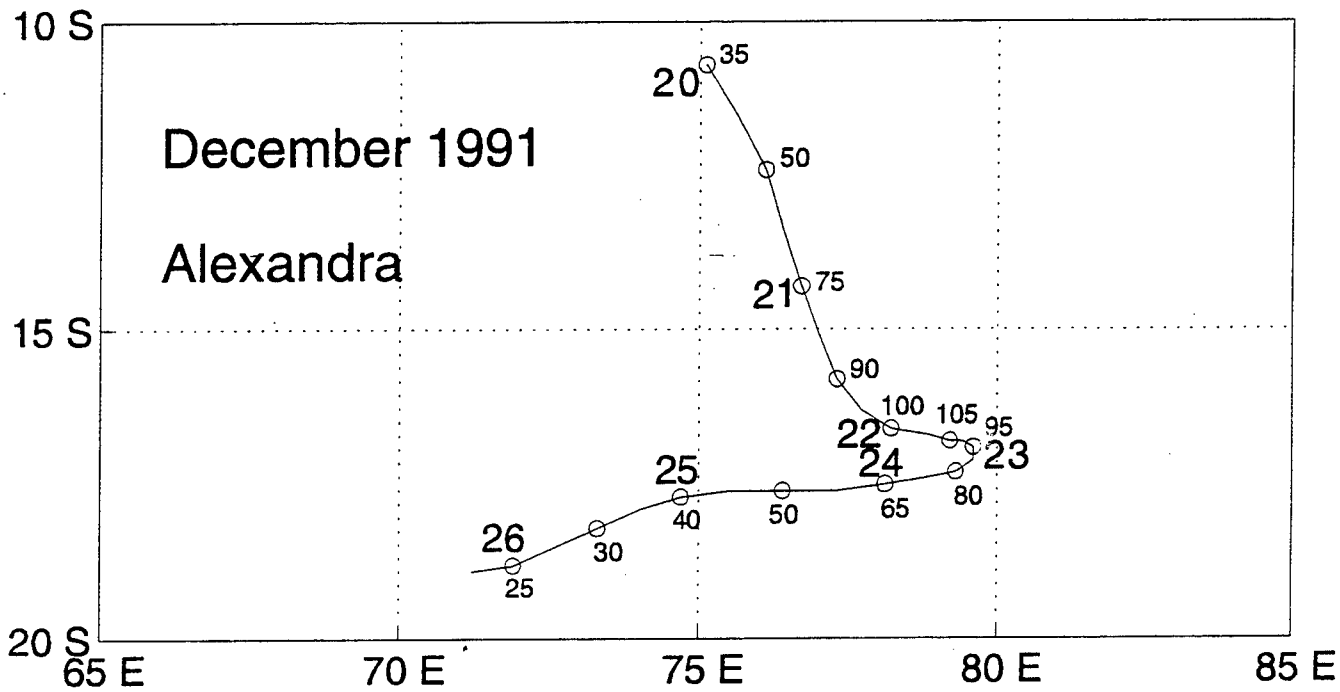

Fig. 22 Best track as in Fig. 11, except for TC Alexandra (0992) during 00 UTC 20 December to 00 UTC 26 December 1991.

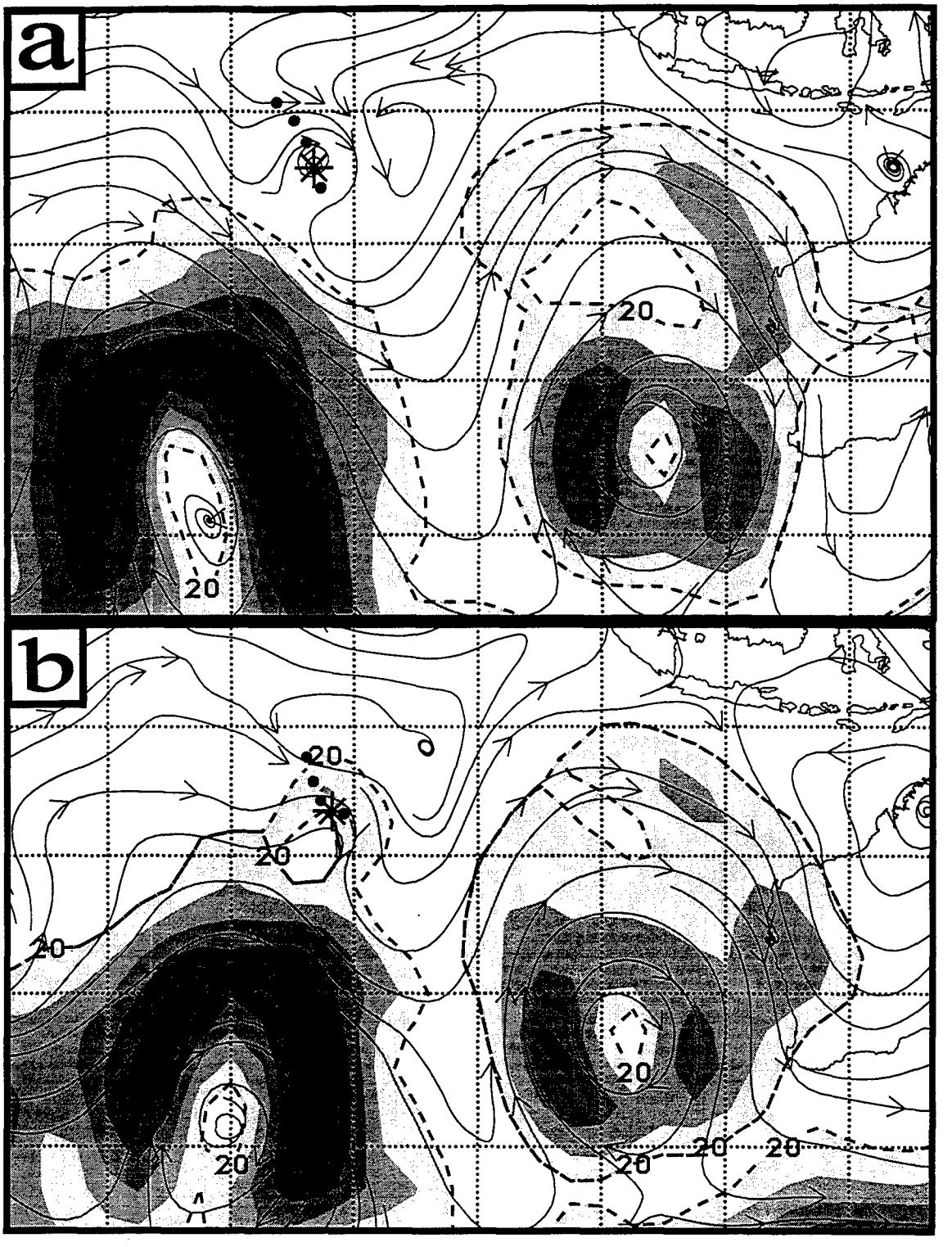

Fig. 23 NOGAPS 500-mb analyses as in Fig. 13, except valid at 00 UTC on (a) 21, (b) 22, (c) 23, and (d) 24 December 1991.

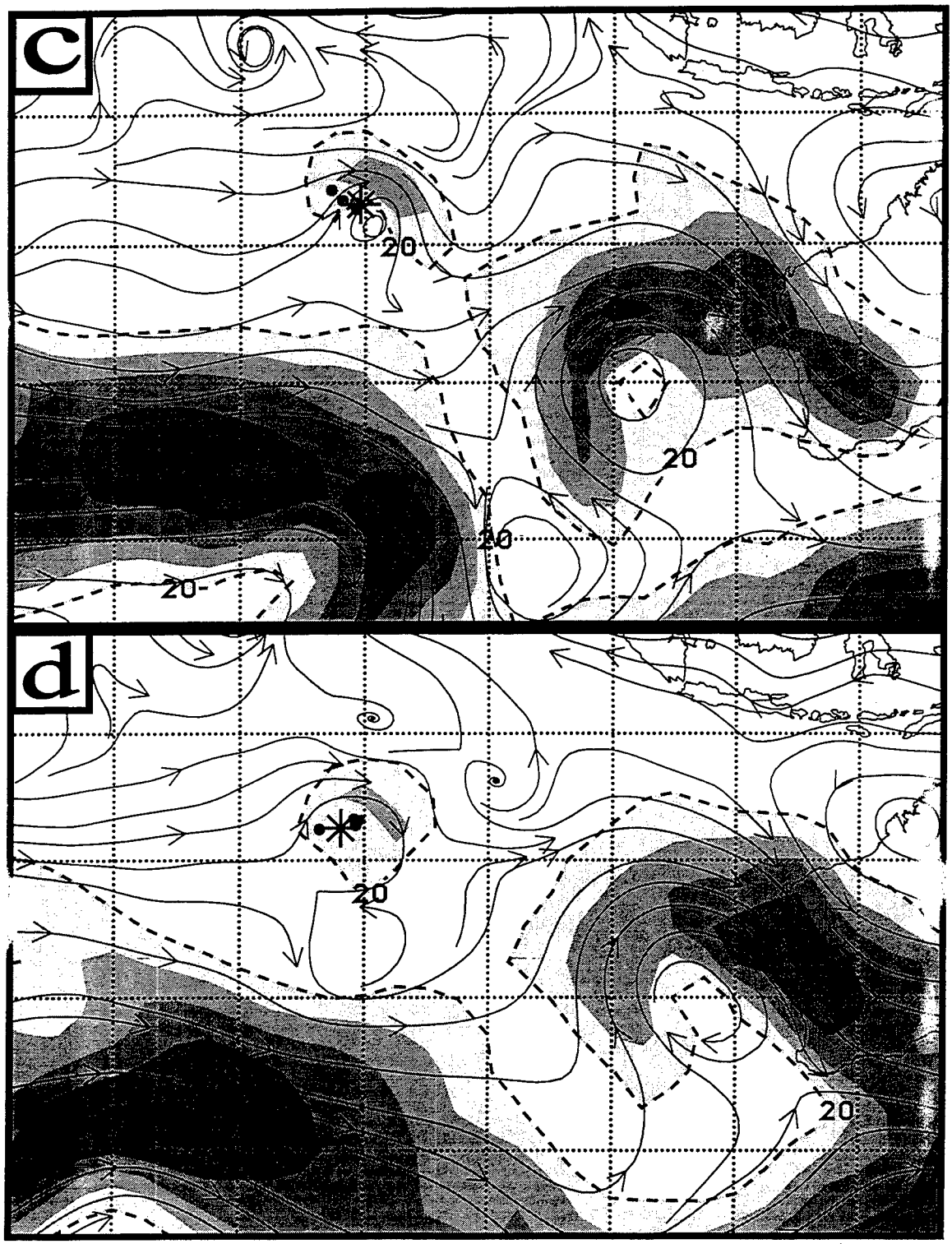

Fig. 23 (continued) NOGAPS 500-mb analyses valid at 00 UTC on (c) 23 and (d) 24 December 1991.

translate toward the cutoff low near Australia, which further compresses the intervening ridge. TC Alexandra is beginning to transition from H/TP to H/EW and turn more eastward as its environmental steering is changed from the northwesterlies ahead of the trough to the weaker westerlies at the equatorward end of this weakening trough. Notice also the isotach maxima around the western trough are greater than in the eastern cutoff. The stronger isotach maximum is on the eastern side of the western trough, which indicates that the trough is beginning to weaken. In the cutoff low near Australia, the stronger isotach maximum is on the western side, which indicates that it is still in a developing stage, probably since the pressure gradient increases as the intervening ridge approaches. The trend continues at 00 UTC 23 December (Fig. 23c) when the western trough has collapsed. With this change in the environmental steering as the midlatitude circulation is becoming more zonal, TC Alexandra has stalled as a transition begins from H/EW to S/DR. Notice that the cutoff near Australia now has an isotach maximum on the equatorward side of the cutoff. With no further injections of energy on the western flank, the cutoff will soon begin to weaken. By 00 UTC 24 December (Fig. 23d), the transition is complete, as TC Alexandra is now in the S/DR pattern/region and is moving west on the equatorial side of a small, growing subtropical anticyclone.

When this example is combined with the SRM-influenced examples in Bannister *et al.* (1997), it reinforces the position that forecasters must be very aware of the phase of the SRM process that is occurring in the midlatitudes. In particular, both an amplification or a weakening of either a trough or a ridge can have an effect on the TC environment via changing pressure gradients.

Thus, monitoring the height tendencies of these circulations at the steering level (typically 500 mb) may provide clues as to the phase of the SRM process. For example,

decreasing 500-mb heights in an approaching midlatitude trough provides an indicator that the trough may amplify sufficiently to affect the environmental steering of the TC via the SRMT process. Similarly, monitoring the 500-mb heights in the adjacent subtropical high pressure cell with time may be another indicator that the situation is changing. When combined with the streamline/isotach analysis as above, the pressure height information can give forecasters an additional indicator that the SRM process may have an effect on the TC motion.

(2) SRM amplifying. This case study is of an amplifying midlatitude trough that causes downstream ridging to the south of TC Betsy, and the changes in the track of Betsy. The track of TC Betsy during 5 January to 10 January 1992 is shown in Fig. 24. A change in track occurs from being toward the south on 7 January to a westward track on 9 January. The first NOGAPS 500-mb analysis (Fig. 25a) has TC Betsy in a P/PO pattern/region with a peripheral ridge and a 20-kt isotach extending from southeast to northeast. Notice the amplifying ridge/trough couplet over southern Australia and the relatively zonal ridge to the southwest of TC Betsy. Twenty-four hours later (Fig. 25b), TC Betsy has begun a transition to the S/DR pattern/region as the ridge builds to the south of TC Betsy in response to the amplifying trough over southeastern Australia. By 12 UTC 9 January (Fig. 25c), the transition to S/DR is complete, as TC Betsy is now moving toward the west-southwest equatorward of the subtropical anticyclone. Thus, a dynamical coupling between the slowly approaching midlatitude trough and the subtropical ridge poleward of TC Betsy has made that ridge more dominant than the peripheral ridge, which still exists but is no longer producing the environmental steering.

e. Vertical wind shear illustration

Although briefly introduced as a transitional mechanism in Bannister et al. (1997), Vertical Wind Shear (VWS) may cause such severe track changes that it warrants more

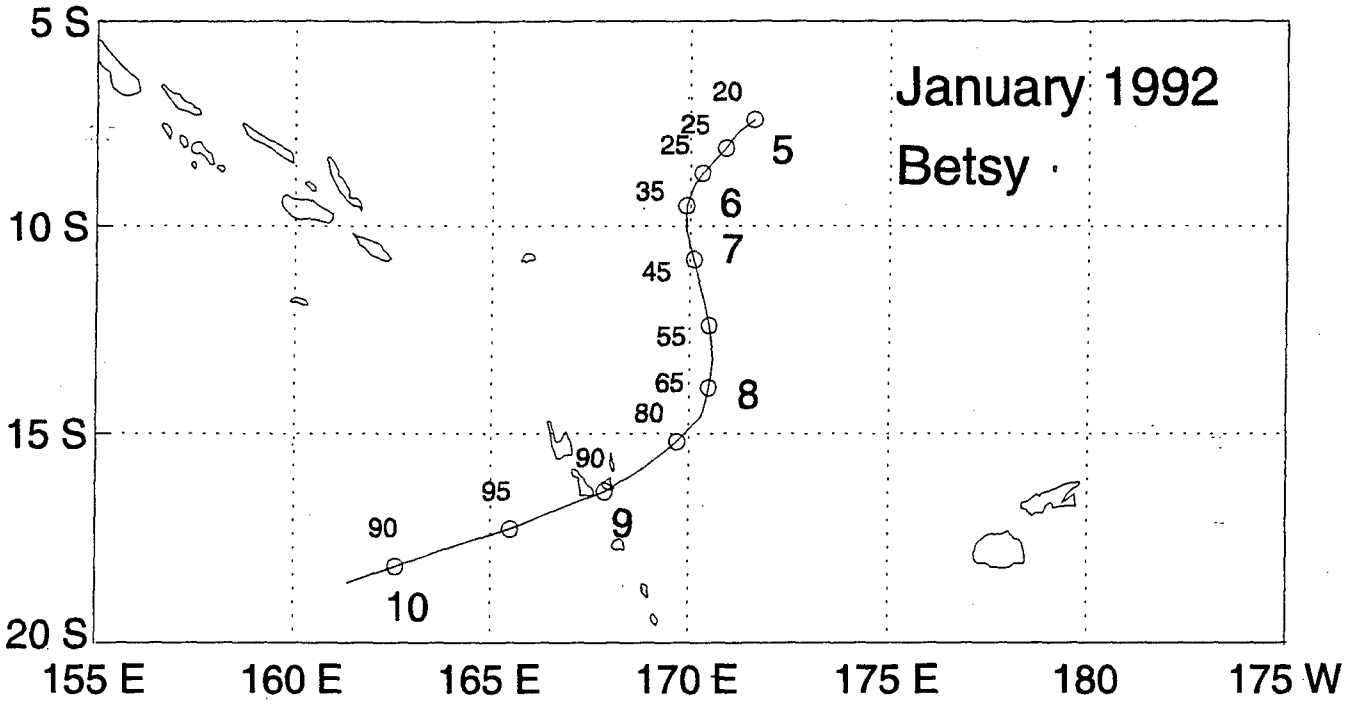

Fig. 24 Best track as in Fig. 11, except for TC Betsy (0392) during 5-10 January 1992.

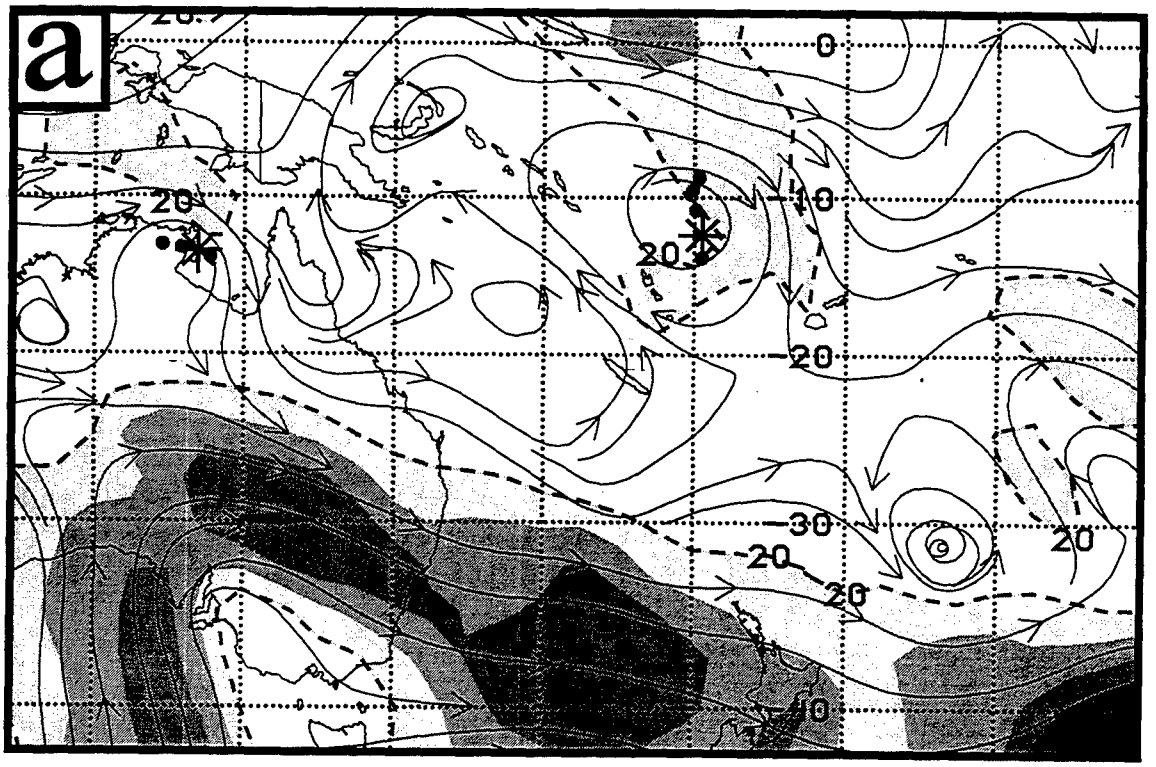

Fig. 25 NOGAPS 500-mb analyses as in Fig. 13, except valid at 12 UTC on (a) 7, (b) 8, and (c) 9 January 1992.

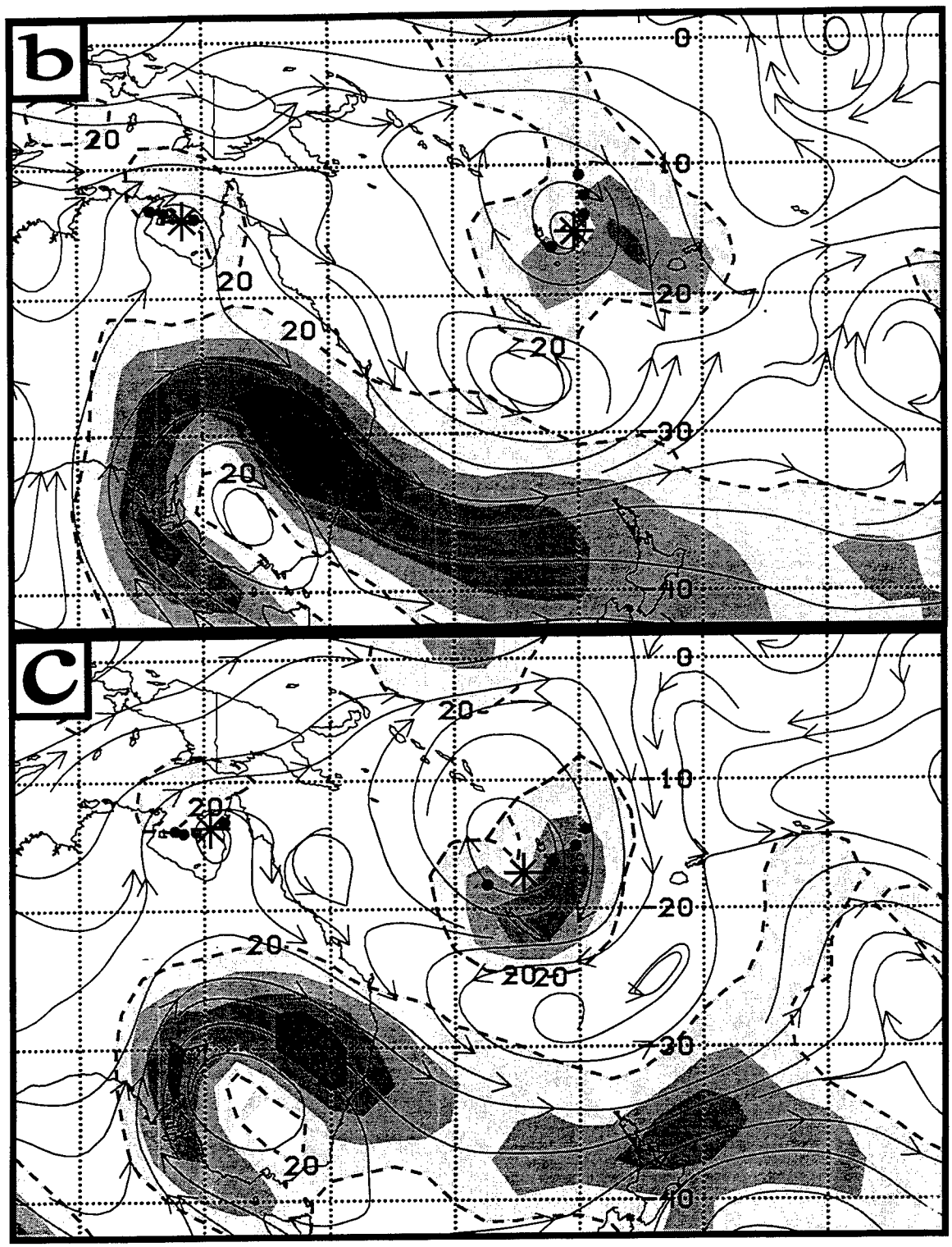

Fig. 25 (continued) NOGAPS 500-mb analyses on (b) 8, and (c) 9 January 1992.

description. Recognition of a VWS event requires that the forecaster be alert to changes in environmental flows at upper and lower levels. The forecaster will then have a better chance at predicting when the TC structure will be changed so that the environmental steering will be at a lower level, and a drastic track change may occur. Such a drastic change of track and the concurrent intensity decrease of TC Tia occurred on 20 November 1991 (Fig. 26). These changes occurred during a VWS event.

The NOGAPS 500-mb analyses for 12 UTC 19 November and 12 UTC 20 November are presented in Fig. 27. In both analyses, TC Tia is near a strong isotach region between a trough to the southwest and a ridge to the northeast. Based on these 500 mb analyses, TC Tia would be categorized as either S/MW (Fig. 2a) or H/TP (Fig. 2c) depending on the forecaster's thoughts on the amplitude of the trough. However, either classification would indicate an eastward component to the track, rather than the northwest direction in which the cyclone is moving at 12 UTC 20 November.

TC Tia's sudden track change becomes much clearer when the upper (200 mb) and lower (850 mb) NOGAPS analyses in Fig. 28 are examined for the same date/time period. Using the same Systematic Approach pattern characterizations at 200 mb, TC Tia would be in the S/MW pattern/region at both times. It is clear that TC Tia has moved into a region of strong westerlies aloft. During the same time period, TC Tia would be classified as being in the H/RE pattern/ region of the ridge to the southwest at the 850 mb level, especially on 20 November when the 30-kt isotach has shifted to south-southwest of Tia and the northwestward environmental steering best agrees with the track.

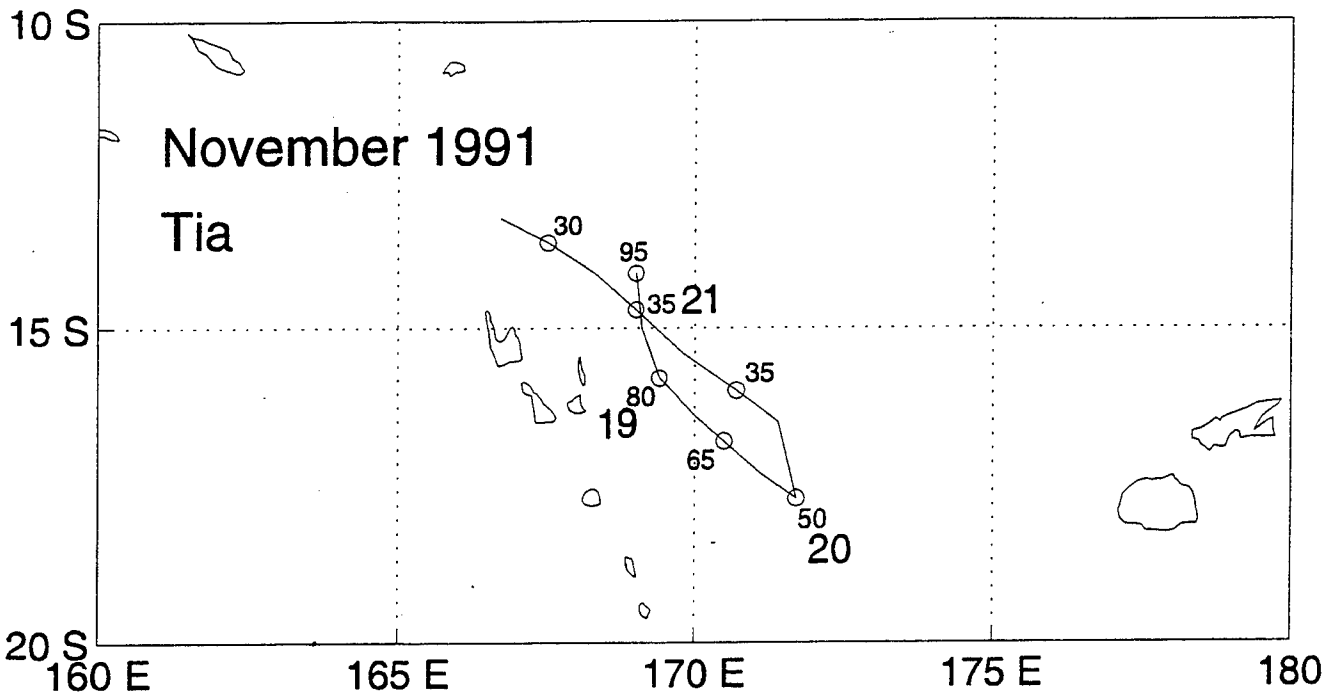

Fig. 26 Best track as in Fig. 11, except for TC Tia (0392) during 12 UTC 18 November to 12 UTC 21 November 1991.

The "storyline" for this event is that TC Tia encountered increasing vertical wind shear as it translated to the poleward side of the upper-tropospheric ridge axis; however, it remained on the equatorward side of the ridge axis at low levels. Owing to the vertical shear early on 20 November, the mid- to upper-level vortex was detached from the low-level center of TC Tia. Thus, Tia began to move with the environmental flow at a lower level, which in this case was southeasterlies due to the influence of the low-level ridge to the southwest of the TC. This vertical wind shear description is consistent with the decrease in intensity on 20 November (Fig. 26). Continued monitoring of the low-level center is essential because of the potential for re-intensification owing to the presence of higher sea-surface temperatures.

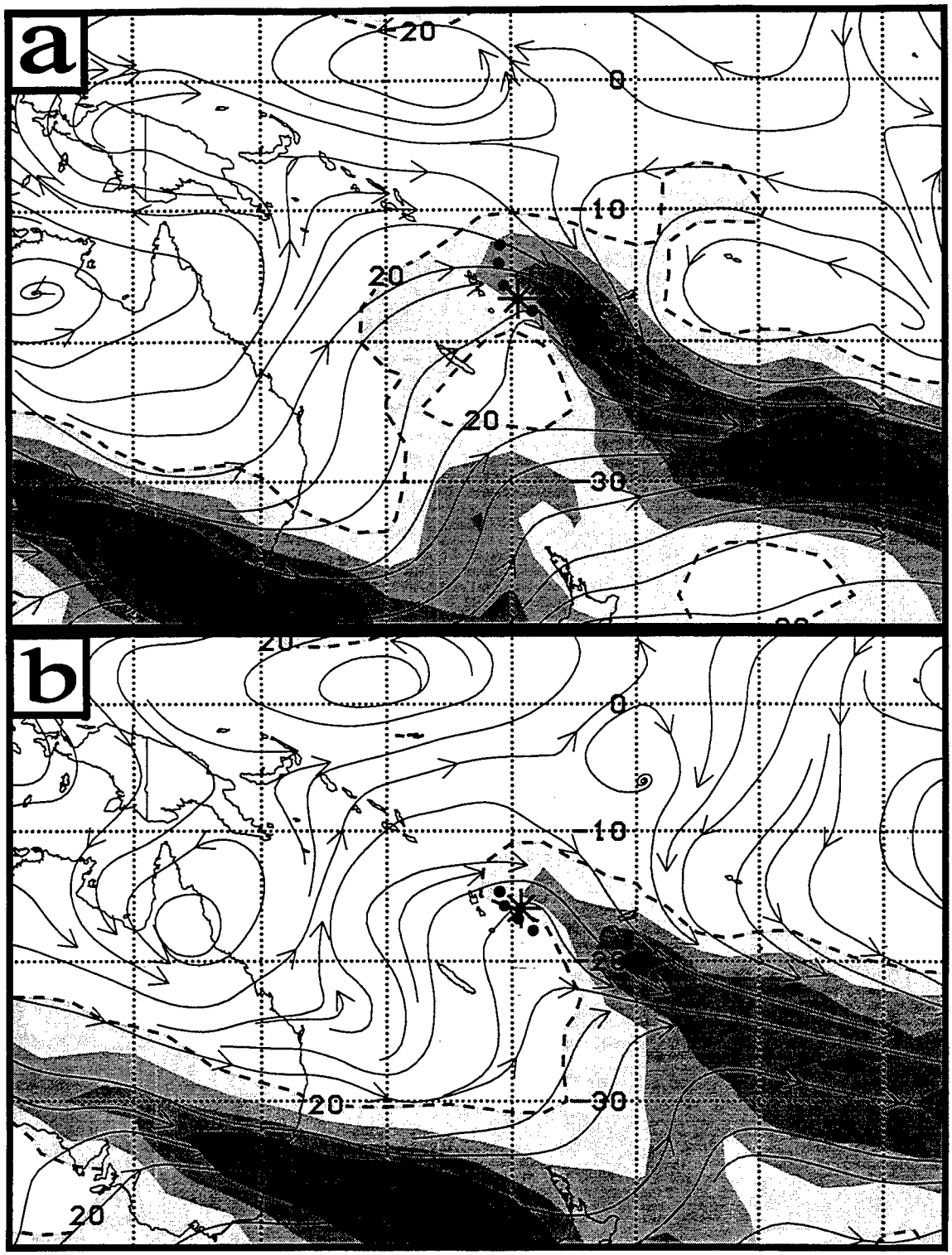

Fig. 27 NOGAPS 500-mb analyses as in Fig. 13, except at 12 UTC on (a) 19 and (b) 20 November 1991.

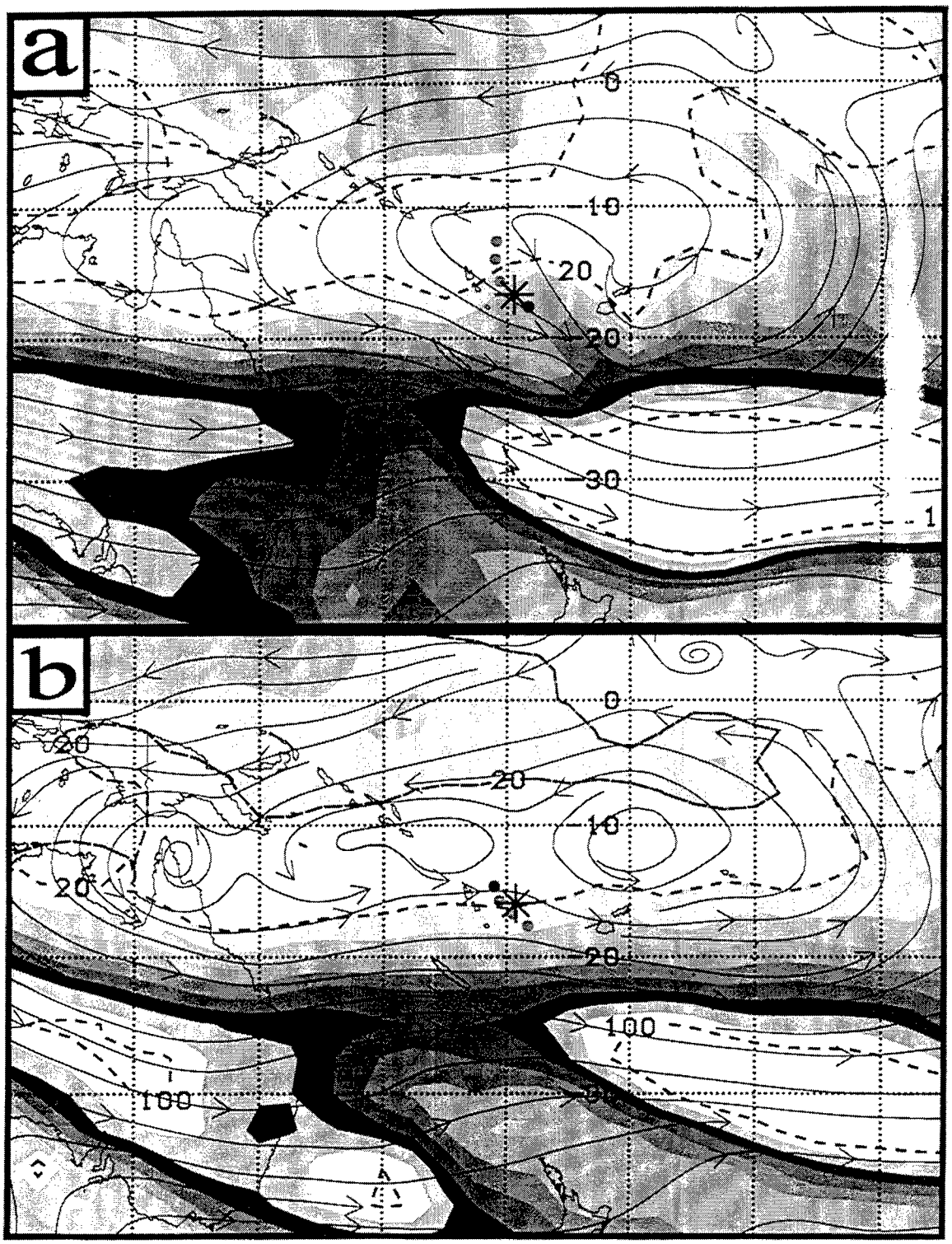

Fig. 28 NOGAPS analyses as in Fig. 13, except at 200 mb for 12 UTC on (a) 19, and (b) 20 November 1991, and at 850 mb in (c) and (d) for the same dates.

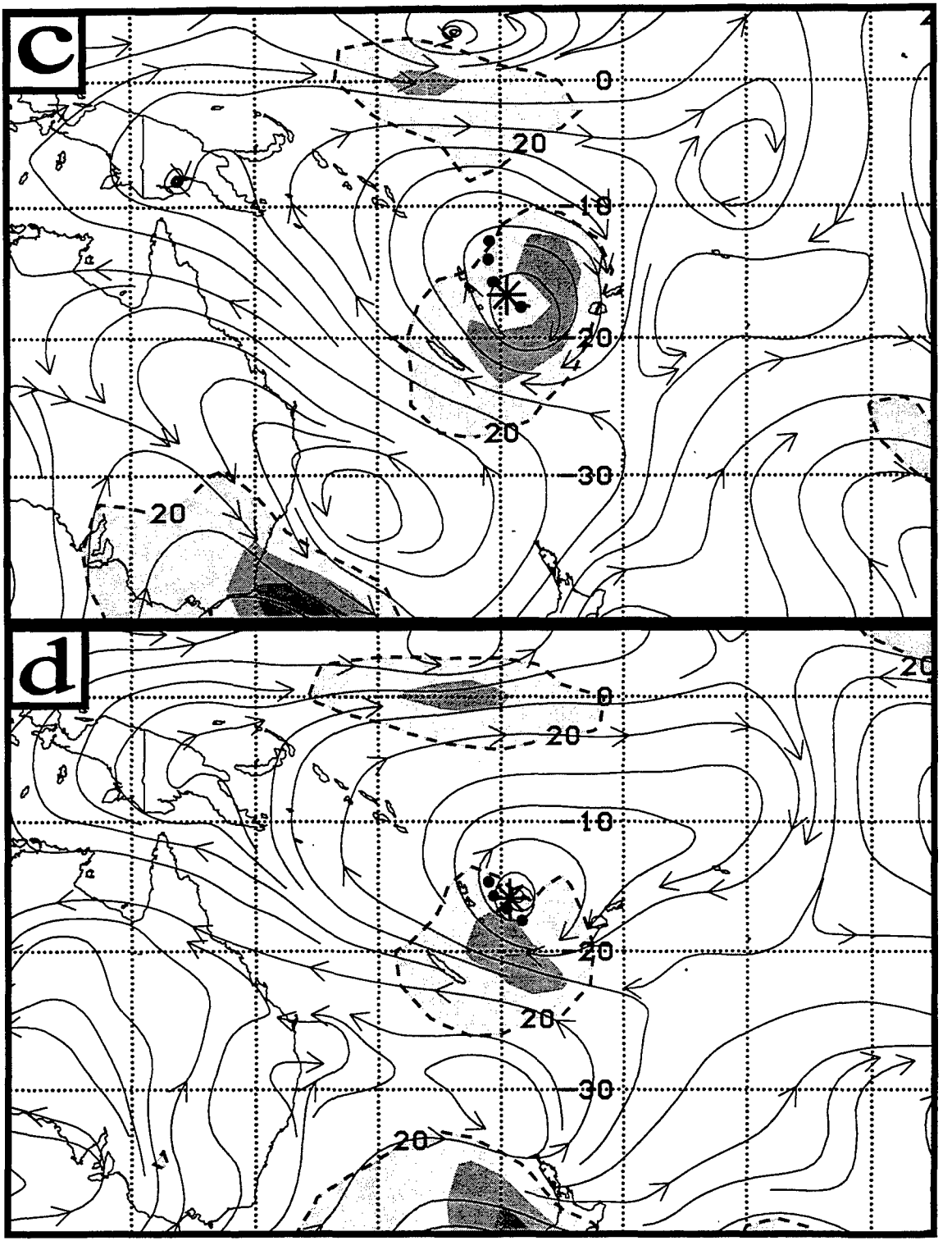

Fig. 28 (continued) NOGAPS 500-mb analyses at 12 UTC on (c) 19 and (d) 20 November 1991.

This case study illustrates that the Systematic Approach can be used to alert the forecaster that a vertical wind shear event may lead to a change in the level at which the environmental steering of the TC will occur. During such a scenario, the forecaster should assess the pattern/region characteristics of the TC at both the upper (around 200 mb) and the lower (around 850 mb) levels of the atmosphere. If the two steering flows are opposed to each other as in this case study with the 200-mb northwesterlies and the 850-mb southeasterlies, he/she should then look for other confirming evidence that vertical shear is in fact occurring. This evidence may include a weakening of the system organization on satellite imagery, a decreased translation of the system, dramatic track changes predicted by the global model, etc. The forecaster then has a much better meteorological basis to decide if a drastic track change should be forecast.

f. Summary

This section has described a number of refinements to the Systematic Approach meteorological knowledge base as it applies in the Southern Hemisphere. These refinements have arisen from the experience gained from a doubling of the SH cyclone data base and increase of the climatology from four years to eight years. A summary of these refinements and how they fit into the meteorological knowledge base is given below:

- Equatorial Westerly Wind Bursts (EWWB) may have an impact on a TC track by extending the time the TC moves to the east, or by establishing an eastward environmental steering that will drastically change the TC track direction from being toward the west in S/DR to toward the east in S/EW. An important indicator of the EWWB event is a characteristic east-west oriented cloud pattern equatorward of the TC in the satellite imagery.
- The important concept implicit in the previous point is that it is critical for the

forecaster to assess environmental steering wind influences in all quadrants of the TC, and particularly the possible effects of increases or decreases in the strength of these steering winds.

- STIQ has been identified as a mechanism to increase the eastward translation of a near-equatorial TC that is between a TC to the south or southeast and the equatorial buffer cell to the north or northwest.

- Although no examples have been found to date, it is conceivable that the westward translation of a poleward TC could be increased due to the STIP process in which the poleward TC is between another cyclone to the north or northwest and the subtropical ridge cell to the south or southeast.

- Subtropical Ridge Modulation (SRM) may involve both the amplification and the weakening of mid-latitude troughs and ridges. It is critical for the forecaster to assess the phase of the SRM process and then the impact of this SRM on the TC motion in the SH.

- The Systematic Approach can be used in a qualitative sense to decide if a TC may be affected by Vertical Wind Shear. Characterizing the pattern/region of the TC at both the upper and lower levels of the atmosphere, combined with careful satellite analysis and numerical model diagnosis, may help the forecaster to anticipate the possibility of a drastic change in the TC track if the warm-core aloft is sheared off and the weakened TC then begins to move with a lower-tropospheric flow in a different direction.

Consequently, the Southern Hemisphere Meteorological Knowledge Base (Bannister *et al.* 1997) has been updated to now appear as Fig. 1.

4. Summary and Conclusion

This study has extended the preliminary adaptation by Bannister *et al.* (1997) of the Systematic Approach to Tropical Cyclone Track Forecasting meteorological knowledge base to the Southern Hemisphere. Inclusion of an additional four years of cases essentially doubled the sample of environment structure classifications. Thus, the total number of synoptic pattern/region classifications is now 3257, with 2123 in the South Indian Ocean and 1134 cases in the South Pacific Ocean. The eight-year sample contains 145 (90) TCs in the South Indian (Pacific) region, which includes seven TCs that crossed 142°E and thus were counted in both regions. An important conclusion is that a "storyline" for every storm track could be described in the context of only four synoptic patterns and 11 synoptic regions.

Although the same general track characteristics are found in the expanded eight-year sample, the coverage is much improved. Inclusion of the 1997-98 El Niño period increased the sample of South Pacific storms and the tracks now extend to 130°W. Thus, the "climatology" of occurrences of cases in each synoptic pattern/region combination (Fig. 4) is improved, although future years should be added to the data base. As long as a TC remains in the environmental steering flow associated with a particular synoptic pattern/region, the TC track will fall within a range of directions and speeds, i.e., a characteristic track. These tracks are updated for the eight-year sample in Sections 2c-2f for the four synoptic patterns. Even though the recurring (greater than three) environment structure transitions that are summarized in Fig. 9 are improved relative to the prior study, additional years should be included in the furture.

Doubling the Southern Hemisphere data base led to some refinements in the set of TC-environment transitional mechanisms in the meteorological knowledge base. A new Equatorial Westerly Wind Burst (EWWB) mechanism has been described and illustrated with three case

studies. This transitional mechanism leads to a low-latitude track reversal from westward to eastward as the wind burst approaches on the equatorward side of the TC. Three case studies illustrating the EWWB mechanism indicate the importance of the TC forecaster monitoring the equatoral westerlies even when the low-latitude TC is moving westward in the tradewind easterlies.

A new semi-direct TC interaction equatorward (STIQ) and poleward (STIP) conceptual model is introduced and an example of the STIQ is shown in which an eastward environmental steering current is enhanced by the increased pressure gradient between the high pressure in an equatorial buffer cell and the low pressure in a poleward TC. Although no TC has yet been labeled as an STIQ case, it is conceivable that a poleward TC may be in an enhanced pressure gradient between the high pressure in the subtropical ridge and the low pressure in an equatorward TC.

The midlatitude westerlies and the subtropical anticyclone in the Southern Hemisphere may be considered to be dynamically linked as troughs intrude equatorward and ridges extend poleward. Whereas Bannister et al. (1997) did describe the Subtropical Ridge Modulation (SRM) transitional mechanism, the eight-year sample re-emphasized the importance of the midlatitude westerlies. Two case studies of a SRM weakening and a SRM amplifying have been included in Section 3d to illustrate the SRM variations. Therefore, the TC forecaster must be alert to midlatitude circulation changes poleward of the TC.

Similarly, the Vertical Wind Shear (VWS) transitional mechanism was described in Bannister et al. (1997). With the vigorous and highly transient midlatitude circulations poleward of Southern Hemisphere TCs, the VWS mechanism should be expected to have a more important role than in (say) the western North Pacific. Thus, a case study is included of a dramatic TC

track change as the upper-tropospheric warm core is advected away and the environmental steering is shifted to a lower level. Thus, the forecaster must be aware of the three-dimensional wind field in the environment of the TC.

APPENDIX

Annual summaries of the synoptic pattern/region assignments for each storm during the 1990-91 through 1993-94 seasons and the 1997-98 season are provided on the following pages. Each entry in the main part of the table shows the number of synoptic times (0000 and 1200 UTC) that the identified TC was classified as being in each of the particular pattern/region combinations appearing at the top of the table. If at a particular time the environment of the TC was considered to be in a transitional state between two pattern/region combinations, each combination was assigned a value of 0.5. This convention accounts for appearance of non-integer values in the tables. The total number of synoptic times for each TC appears in the far right column labeled DTG. Summary statistics for the year and for the entire four-year data base are provided at the bottom of each table.

1990-91		S				P	H				M		
#	STORM	EW	DR	WR	MW	PO	RP	RE	EW	TP	EF	PF	DTG
1S	01S												
2S	02S												
3P	Sina												
4S	04S												
5S	Laurence												
6P	Joy												
7S	Alison		3.5			7				1.5			12
8S	Bella	0.5	18	2		15.5							36
9S	Chris	3.5	10.5										14
10S	Cynthia					5							5
11S	Daphne	1.5	10				3.5						15
12S	Debra		1	9	3.5		1			2.5			17
13P	Kelvin	11.5	9.5										21
14S	Elma	3	2			7							12
15P	15P		3.5	1.5									5
16P	16P		3.5			7.5							11
17S	Fatima		13			8.5				2.5			24
18S	Errol		8.5	2.5					3	2			16
19S	Marian	1.5	14	1			2.5						19
20S	Fifi			0.5						8.5	3		12
21P	Lisa			4	8								12
22S	Gritelle		9	3									12
23													
24													
25													
26													
27													
28													
29													
30													
31													
32													
33													
34													
35													
36													
37													
38													
90-91	REGIONS	21.5	106	23.5	11.5	50.5	7		3	17	3		243
	%	8.8	43.6	9.7	4.7	20.8	2.9		1.2	7	1.2		100
	PATTERNS		162.5			50.5		27			3		
	%		66.9			20.8		11.1			1.2		
91-98	REGIONS	265	1354	183	220.5	619	125.5	68.5	135	246	17	24	3257
	%	8.1	41.6	5.6	6.8	19	3.9	2.1	4.1	7.5	0.5	0.7	100
	PATTERNS		2022.5			619		574.5			41		
	%		62.1			19		17.6			1.3		

1991-92		S				P	H				M		
#	STORM	EW	DR	WR	MW	PO	RP	RE	EW	TP	EF	PF	DTG
1S	01S			1.5	2.5			2					6
2S	02S		11	0.5				3.5					15
3P	Tia	7.5	3.5	0.5	3		2	1.5					18
4S	04S		4.5	1.5		4							10
5S	Graham	8.5	3	4.5		3							19
6P	Val	9.5	1			1.5				5.5	1.5		19
7P	Wasa	8	0.5	4								3.5	16
8P	Arthur	2							3				5
9S	Alexandra		6.5						4.5	5			16
10S	Bryna		6										6
11P	Betsy		8		3.5	9.5							21
12P	Mark	5.5							2.5				8
13P	13P									1			1
14P	Cliff				2.5	5			1.5				9
15S	Celesta							3		4			7
16S	16S		2										2
17P	Daman		5.5		2		5.5						13
18P	18P		1.5				1.5						3
19S	Davilia				5								5
20S	Harriet		17			6				3			26
21P	Esau		3.5			14.5		5					23
22S	Farida		16.5	1.5									18
23S	Ian		2.5			5	1.5	1	3	2			15
24S	Gerda	2	4.5			4.5							11
25P	Fran		19	1	2.5	1.5							24
26P	Gene		0.5			8			2.5				11
27P	Hettie			3	3.5					3.5			10
28S	Neville	1.5	6.5	12									20
29S	Jane/Ima		11.5	0.5	5	7							24
30P	Innis		3.5	2.5	1.5					2.5			10
31													
32													
33													
34													
35													
36													
37													
38													
91-92	REGIONS	44.5	138	33	31	69.5	10.5	16	17	26.5	1.5	3.5	391
	%	11.4	35.3	8.4	7.9	17.8	2.7	4.1	4.3	6.8	0.4	0.9	100
	PATTERNS		246.5			69.5		70			5		
	%		63			17.8		17.9			1.3		
91-98	REGIONS	265	1354	183	220.5	619	125.5	68.5	135	245.5	17	24	3257
	%	8.1	41.6	5.6	6.8	19	3.9	2.1	4.1	7.5	0.5	0.7	100
	PATTERNS		2022.5			619		574.5			41		
	%		62.1			19		17.6			1.3		

1992-93		S				P	H				M		
#	STORM	EW	DR	WR	MW	PO	RP	RE	EW	TP	EF	PF	DTG
1S	Aviona	1.5	7.5	3									12
2S	Babie		4	4									8
3P	Joni		4.5			10				2.5			17
4S	04S		16										16
5S	Ken		11	1									12
6P	Nina	14	0.5						11.5				26
7P	Kina	7	5.5						4	4.5			21
8P	08P									4			4
9P	09P		3.5							2.5			6
10S	Colina		11.5			7.5							19
11S	Dessilia			1	3.5	2.5							7
12S	Edwina		10			5.5	8.5						24
13S	Lena	9	8.5				4.5						22
14P	14P	0.5	27.5										28
15P	Lin								2.5	7.5			10
16P	Oliver	3.5	2			11		3.5					20
17P	Mick		3.5				4.5						8
18P	Nisha				6.5	3.5							10
19S	Finella					8							8
20P	Oli								1.5	5.5			7
21P	Polly		0.5	4	8					5.5			18
22P	Roger		1.5				9.5	3.5	5	2.5			22
23P	Prema		5.5	4						5.5			15
24S	Jourdanne		7.5	2	6.5								16
25S	Monty		2	1.5	2					1.5			7
26S	Konita	1.5	7.5			4							13
27P	Adel		7										7
28													
29													
30													
31													
32													
33													
34													
35													
36													
37													
38													
92-93	REGIONS	37	147	20.5	26.5	52	27	7	24.5	41.5			383
	%	9.7	38.4	5.4	6.9	13.6	7	1.8	6.4	10.8			100
	PATTERNS		231			52		100					
	%		60.3			13.6		26.1					
91-98	REGIONS	265	1354	183	220.5	619	125.5	68.5	135	246	17	24	3257
	%	8.1	41.6	5.6	6.8	19	3.9	2.1	4.1	7.5	0.5	0.7	100
	PATTERNS		2022.5			619		574.5			41		
	%		62.1			19		17.6			1.3		

1997-98		S				P	H				M		
#	STORM	EW	DR	WR	MW	PO	RP	RE	EW	TP	EF	PF	DTG
1S	01S	4	7										11
2P	Lusi		1			4				4			9
3P	03P			4.5						2.5			7
4P	Martin		4.5	1.5	3.5					4.5			14
5P	Nute		4				2						6
6P	Osea		3	1.5						6.5			11
7P	Pam	4			2.5	5		2.5					14
8S	Sid	4	2										6
9S	Selwyn	0.5	8				4.5						13
10P	Ron	0.5	9			5.5							15
11P	Susan	3	21	1.5						6.5			32
12P	Katrina	15	12.5	3.5		4		8.5	4.5				48
13S	13S		3	1.5	7.5								12
14P	Les		11.5			3.5		2					17
15S	Tiffany		18										18
16P	Tui									5			5
17P	Ursula									3			3
18P	Veli									7			7
19P	Wes								9				9
20S	Anacelle		5.5		3.5	9							18
21/23S	Beltane		1		9	15.5		2.5					28
22S	Victor/Cindy		23	2									25

24S	24S		2		1	3							6
25P	May					4.5		2.5					7
26S	Donaline					7.5			3.5				11
27S	Elsie		7	4.5	1		3.5						16
28S	Fiona		3.5			6.5				2			12
29P	Yali		10	1	6.5	2.5							20
30P	Nathan	12	11										23
31P	Zuman	1	9.5	1.5	1.5	1				2.5			17
32S	Gemma	7.5	7					0.5	3				18
33S	33S								3				3
34S	34S		11										11
35	35S		3.5			3.5							7
36P	Alan			3.5				3		6.5			13
37P	Bart				2								2
97-98	REGIONS	51.5	199	26.5	38	75	10	21.5	23	50	0	0	494
	%	10.4	40.2	5.4	7.7	15.2	2	4.4	4.7	10.1	0	0	100
	PATTERNS		314.5			75		104.5			0		
	%		63.7			15.2		21.2			0		
91-98	REGIONS	265	1354	183	220.5	619	125.5	68.5	135	245.5	17	24	3257
	%	8.1	41.6	5.6	6.8	19	3.9	2.1	4.1	7.5	0.5	0.7	100
	PATTERNS		2022.5			619		574.5			41		
	%		62.1			19		17.6			1.3		

REFERENCES

Bannister, A. J., M. A. Boothe, L. E. Carr, III, and R. L. Elsberry, 1997: Southern Hemisphere application of the systematic approach to tropical cyclone track forecasting. Part I. Meteorological knowledge base. Tech. Rep. NPS-MR-98-001, Naval Postgraduate School, Monterey, CA 93943-5114, 96 pp.

Boothe, M. A., 1997: Extension of systematic approach to tropical cyclone track forecasting in the eastern and central Pacific. M.S. Thesis, Naval Postgraduate School, Monterey, CA 93943-5114, 134 pp.

Carr, L. E., III, and R. L. Elsberry, 1994: Systematic and integrated approach to tropical cyclone track forecasting. Part I. Approach overview and description of meteorological basis. Tech. Rep. NPS-MR-94-002, Naval Postgraduate School, Monterey, CA 93943-5114, 273 pp.

Carr, L. E., III, and R. L. Elsberry, 1998: Objective diagnosis of binary tropical cyclone interaction for the western North Pacific Basin. *Mon. Wea. Rev.*, **126**, 1737-1740.

Carr, L. E., III, M. A. Boothe, and R. L. Elsberry, 1997: Observational evidence for alternate modes of track-altering binary tropical cyclone scenarios. *Mon. Wea. Rev.*, **125**, 2094-2111.

DISTRIBUTION LIST

Space and Naval Warfare Systems Command PMW 185 4301 Pacific Highway San Diego, CA 92110-3127	5
Dr. Carlyle H. Wash, Chairman Department of Meteorology, MR/Wx 589 Dyer Rd., Room 254 Monterey, CA 93943-5114	1
Dr. Russell L. Elsberry Department of Meteorology, MR/Es 589 Dyer Rd., Room 254 Monterey, CA 93943-5114	90
Library, Code 0142 Naval Postgraduate School Monterey, CA 93943	2
Dean of Research, Code 09 Naval Postgraduate School Monterey, CA 93943	1
Defense Technical Information Center Cameron Station Alexandria, VA 22304-6145	2